

Materials and Methods

Cell lines and clinical PC tissues. COS7 cell and four PC cell lines (LNCaP, 22Rv1, PC-3, and DU-145) were purchased from the American Type Culture Collection (ATCC, Rockville, MD, USA). They were grown in Delbecco's modified Eagle's medium with or without phenol red (Invitrogen, Carlsbad, CA, USA); these media were supplemented with 10% fetal bovine serum (FBS) or 10% charcoal/dextran-treated FBS (Hyclone, Logan, UT, USA) and 1% antibiotic/antimycotic solution (Sigma-Aldrich, St. Louis, MO, USA). Cells were maintained at 37°C in atmospheres of humidified air with 5% CO₂. Clinical CRPC tissues were obtained by autopsy and transurethral resection of prostate (TURP) at Kochi University Medical School, Iwate Medical University, Kyoto Prefectural University of Medicine, and Okayama University Medical School with the appropriate informed consents, as described before,⁽¹²⁾ and the tissues included one liver metastasis, two lymphnode metastases, and two bone metastases from autopsies. All patients were undergoing the treatment of LH-RH agonist even after the emergence of CRPC.

Steroid compounds. Steroid compounds used in this study were purchased from Sigma or Steraloids (Newport, RI, USA) and included: androstenedione (Sigma), cholestanone (Steraloids), 5 α -dihydrocorticosterone (Steraloids), 5 α -dihydrocortisone (Steraloids), 5 α -dihydroprogesterone (Sigma), 5 α -dihydroDOC (Steraloids), 5 α -dihydrocortisol (Steraloids), 5 α -dihydro-17OH-progesterone (Steraloids), corticosterone (Sigma), cortisone (Sigma), progesterone (Sigma), DOC (Sigma), cortisol (Sigma). All steroids were dissolved by pure ethanol.

MTT (3-[4,5-dimethylthiazol-2-yl]-2,5-diphenyltetrazolium bromide) assays. Prostate cancer (PC) cells were cultured in the medium containing 10% charcoal/dextran-treated FBS. Cell proliferation assay was performed by plating 1.5×10^5 of 22Rv1 cells, 2.0×10^5 of LNCaP cells, 4.0×10^4 of DU-145 cells, or 5.0×10^4 of PC-3 cells on six-well plates. Twenty-four hours later, cells were treated with the indicated concentration of each steroid and cultured for additional 72 h. Cell viability was measured by MTT assay using Cell-Counting kit-8 (Dojindo, Kumamoto, Japan). Absorbance at 490 nm and at 630 nm as a reference was measured with a multi-label counter ARVO MX (Perkin Elmer, Fremont, CA, USA). Each experiment was performed six times.

Dual luciferase assays. Twenty-four hours after plating 3×10^5 cells of 22Rv1, DU-145, and PC-3 or 5×10^5 cells of LNCaP on six-well plates in the media with 10% charcoal/dextran-treated FBS, 22Rv1, DU-145, or PC-3 cells were co-transfected by FuGENE6 (Roche, Basel, Switzerland) with 0.5 μ g of pGL3-PSA luciferase reporter plasmid and 0.1 μ g of *Renila* luciferase expression plasmid serving as an internal control. As for LNCaP, Lipoectamine 2000 (Invitrogen) was used as a transfection reagent. Human AR expression plasmid pSG5-AR (wild type), pSV-ARmut T877S, or mock vector (provided by Dr. Chang at University of Rochester Medical Center) was co-transfected to PC-3 cells, and 24 h after transfection, cells were treated with the indicated concentration of each steroid. Cells were harvested 48 h after addition of the steroid and lysed by the lysis buffer (Dual-Luciferase Reporter Assay System; Promega, Madison, WI, USA). The luciferase activity was quantified by a luminometer, and the results were normalized by *Renila* luciferase activity. To examine the specificity of AR activation by each steroid, 10 μ M of bicalutamide (Sigma-Aldrich) was added 30 min before the cells were treated with each steroid.

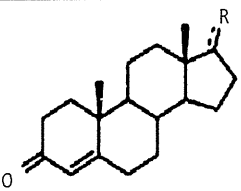
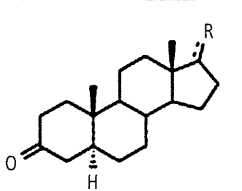
Small-interfering RNA (siRNA) to *SRD5A1*. To inhibit *SRD5A1* expression in PC cells efficiently and specifically, we synthesized RNA duplexes corresponding to the target sequence of *SRD5A1* (siSRD5A1: 5'-GAGCCAUUGUGCAGUGUAUTT-3'

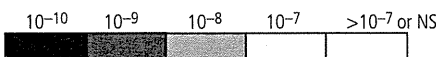
and 5'-AUACACUGCACAAUGGCUCTT-3'), as well as control RNA duplex (siEGFP: 5'-GAAGCAGCAGCAGCUUCUUC-TT-3' and 5'-GAAGAAGUCGUGCUGCUUCTT-3'). 1.8×10^6 of 22Rv1 cells onto a 10-cm dish were transfected with a final concentration of 100 nmol/L of RNA duplex using Lipofectamin RNAiMAX (Invitrogen) according to the manufacturer's instructions. Forty-eight hours after transfection, total RNAs were extracted from the transfected cells to evaluate the knock-down effects by semi-quantitative RT-PCR. The primer sequences were 5'-TTGGCTTGACTCAGGATTTA-3' and 5'-ATGCTATCACCTCCCCTGTG-3' for β -actin (*ACTB*) as an internal control; 5'-CCTGTTTGTCTTTGTTGATTGAA-3' and 5'-CCAGATGAGATGATAAGGCAAAG-3' for *SRD5A1*; and 5'-TTTAATCAGGCCCTGTCTGC-3' and 5'-GGGGTATAGAAATGGAATGGAGA-3' for *SRD5A3*. Forty-eight hours after transfection, MTT assays were performed as described above. For 5 α -steroid reductase assay *in vitro*, 48 h after transfection, the cells were treated with 10^{-6} M DOC, and after 1 h of incubation, their conditioned media were collected to measure their 5 α DH-DOC levels by liquid chromatography-tandem mass spectrometry (LC-MS/MS) as described below.

***In-vivo* 5 α -steroid reductase reaction.** To construct the expression vectors for *SRD5A1* and *SRD5A3*, the entire coding sequences of *SRD5A1* (GenBank accession no. NM_001047) and *SRD5A3* (GenBank accession no. NM_024592) were amplified by PCR using Prime STAR DNA polymerase (Takara, Kyoto, Japan). COS7 cells were transfected with each of HA-tagged expression vectors (*SRD5A1*, *SRD5A3*, and mock). The expressions of exogenous *SRD5A1* and *SRD5A3* were evaluated by western blot analysis using anti-HA tag antibody (Sigma-Aldrich). Forty-eight hours after the transfection, cells were treated with 10^{-6} M DOC, and after 1 h of incubation, the conditioned media were harvested. 5 α -Dihydro-deoxycorticosterone (5 α DH-DOC) levels were measured by LC-MS/MS described below. To inhibit 5 α -steroid reductase activity, we added 1 μ M dutasteride (provided by GlaxoSmithKline, Middlesex, UK) to the media 30 min before DOC treatment.

Quantitative analysis of 5 α DH-DOC and DHT by LC-MS/MS. 5 α -Dihydrotestosterone (DHT) measurement by LC-MS/MS was described previously.⁽¹¹⁾ One ng of DHT-d3 [17,16,16-²H₃]-DHT and 1 ng of Corticosterone-d8 as an internal standard was added to the individual homogenized cells or the conditioned media, which was extracted with ether. The organic layer was evaporated and the extracts were dissolved in 1 mL of 20% acetonitrile-H₂O in an ultrasonic bath and applied to a 3-mL Bond Elut C18 cartridge column (Varian, Harbor City, CA, USA). These columns were then washed successively with 1 mL water and 3 mL of 30% acetonitrile-H₂O, and the steroidal fraction was eluted with 2.5 mL of 70% acetonitrile-H₂O and dried using a centrifugal evaporator. To increase the sensitivity of MS analysis, the dried steroidal fraction was reacted with 50 μ L reagent mixture (50 mg 2-methyl-6-nitrobenzoic anhydride, 20 mg 4-dimethyl-aminopyridine, and 50 mg picolinic acid in 1 mL tetrahydrofuran) and 15 μ L triethylamine for 60 min at room temperature. The reaction mixture diluted with 1% acetic acid was applied to a 3-mL Bond Elut C18 cartridge column. The columns were washed with distilled water and 30% acetonitrile-H₂O, and the steroidal fraction was eluted with 3 mL of 70% acetonitrile-H₂O. The collected fraction was evaporated and dissolved in 100 μ L of 40% acetonitrile-H₂O. Ten millilitres was applied to the LC-MS/MS instrument: API4000 QTRAP (Applied Biosystems, Foster City, CA, USA) equipped with an ESI ion source and a Shimadzu high-performance liquid chromatography (HPLC) system (Shimadzu, Kyoto, Japan). The HPLC column was a Cadenza CD-C18 (150 \times 2 mm, inner diameter 3 μ m; Imtakt, Kyoto, Japan). The mobile phase consisting of acetonitrile-methanol (50:50 v/v, solvent A) and 0.1% formic acid (solvent B) was

Table 1. Summary of the growth-promoting effects of eight 5 α DH steroids and their precursors

									
4-ene-3-oxosteroid	22Rv1	LNCaP	DU1-45	PC3	5 α -DH-3-oxosteroid	22Rv1	LNCaP	DU-145	PC3
Androstenedione					Androstenedione				
Cholestenone					5 α -Dihydrocholestanone				
Corticosterone					5 α -Dihydrocholestanone				
Cortisone					5 α -Dihydrocortisone				
Progesterone					5 α -Dihydrocholestanone				
DOC					5 α -DihydroDOC				
Cortisol					5 α -Dihydrocortisol				
17OH-progesterone					5 α -Dihydro-17OH-progesterone				



The gradient color in each column indicates the concentration of each steroid which shows a statistically significant growth-promoting effect on prostate cancer cells. White indicates a statistically significant growth-promoting effect at the concentration of 10^{-6} or not significant (NS). DOC, 11-deoxycorticosterone.

used with a gradient elution of A:B = 60:40–100:0) at a flow rate of 0.4 mL/min. The electrospray (ESI)/MS conditions were as follows: spray voltage, 3300V; Collision gas, 1.5 psi (gas pressure) nitrogen; curtain gas nitrogen, 11 psi (gas pressure); ion source temperature, 600°C; and ion polarity, positive. For 5 α DH-DOC determination, m/z 333.3 was activated as a precursor ion, and the product m/z 279.2 ions were monitored. The produced ion mass monitored for the internal standards was m/z 125.1. The assay was validated to ensure that the result was within the 20% range of accuracy and precision. The lower limit value for 5 α DH-DOC was 1 pg.

Results

5 α DH Steroids stimulated PC cell growth. For this analysis, we selected eight 5 α -DH-oxosteroids (5 α DH steroids) that were reported to be present naturally in the human body (Table 1). To investigate whether they could stimulate PC cell proliferation, we treated four sets of PC cell lines (22Rv1, LNCaP, DU-145, and PC-3) with serial concentration of eight 5 α -DH-oxosteroids. Simultaneously, we treated the four PC cell lines with their precursors 4-ene-3-oxosteroids, which were expected to be converted to 5 α -DH-oxosteroids by endogenous 5 α -steroid reductases in PC cells, and examined their growth-promoting effect in the same way. As shown in Figure 1a,c treatment of 5 α DH-DOC and 5 α DH-progesterone at 10^{-7} M or lower concentration showed some growth-promoting effect on both 22Rv1 and LNCaP cells which expressed AR, but not on

DU-145 and PC-3 cells which did not express AR. Their precursor steroids (DOC and progesterone) also showed significant growth-promoting effect on AR-positive 22Rv1 and LNCaP cells, but not on AR-negative PC-3 and DU-145 cells (Fig. 1b,d). These findings indicate that 5 α DH-DOC and 5 α DH-progesterone could be good candidates to stimulate PC proliferation through AR activation. On the other hand, corticosterone and cortisol had a positive effect in proliferating cells of AR-negative DU-145, as well as LNCaP or 22Rv1 cells (Fig. S1a,c), and this effect on AR-negative DU-145 cells might be mediated by other steroid receptors, rather than AR. Their 5 α DH steroids did not show any significant growth-promoting effect on PC cell lines (Fig. S1b,d). These data are summarized in Table 1.

5 α -Dihydro-deoxycorticosterone (5 α DH-DOC) activated wild-type AR more efficiently than DOC. Focusing on 5 α DH-DOC and 5 α DH-progesterone, to evaluate their direct ability to stimulate AR transactivation activity, we transfected LNCaP cells and 22Rv1 cells with a luciferase plasmid (pGL3-PSA) driven by the PSA enhancer which included androgen response elements, and compared the luciferase activity reflecting AR transactivation activity by the treatment of these 5 α DH-steroids and their putative precursors. LNCaP cells and 22Rv1 cells expressed mutant AR (T877A and H874Y, respectively) and mutant AR has been reported to respond to steroids differently from wild-type AR.^(14,15) Then, to evaluate their effects on wild-type AR, we also co-transfected AR-null PC-3 cells with wild-type AR or mutant AR (T877S) and examined the transactivation activity of

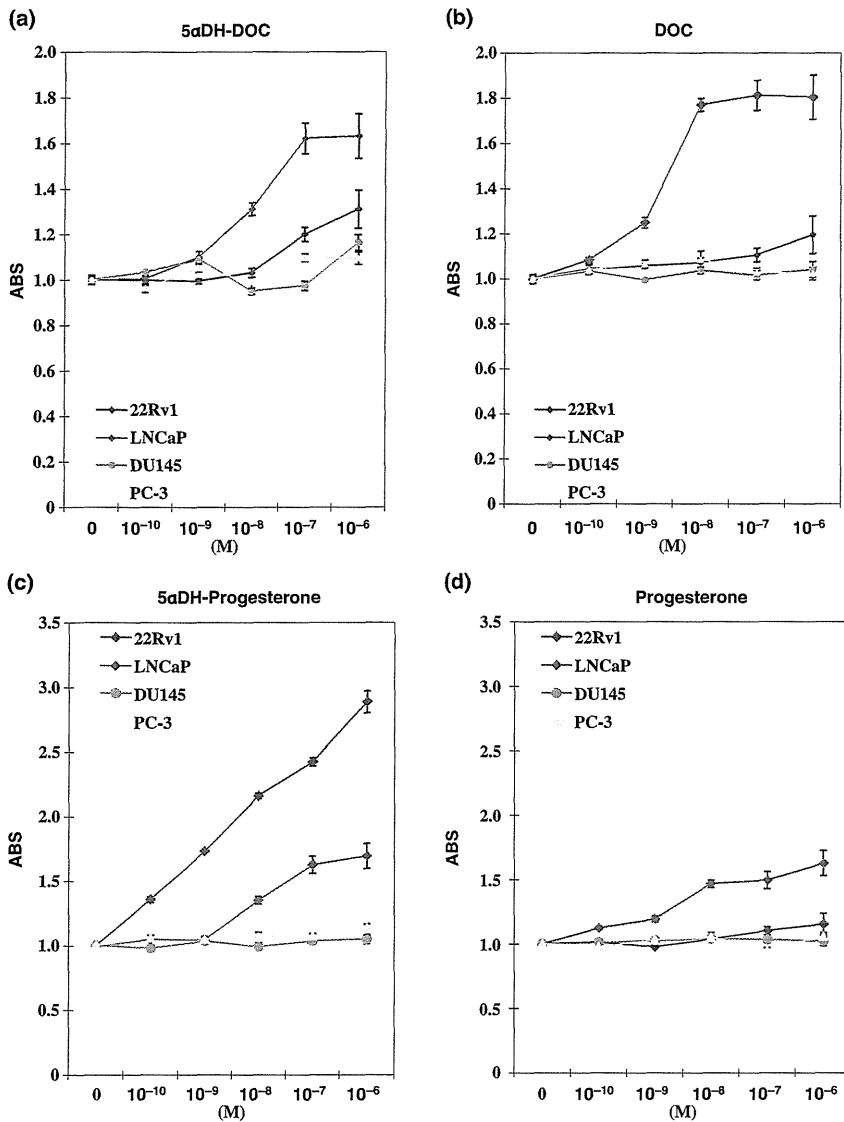


Fig. 1. Cell growth assays of 5 α DH steroids and their precursors. 5 α -Dihydro-deoxycorticosterone (5 α DH-DOC) (a) and 5 α DH-progesterone (c) at 10⁻⁷ M or lower concentration showed growth-promoting effect on both androgen receptor (AR)-positive prostate cancer (PC) cell lines 22Rv1 and LNCaP, but did not on AR-negative PC cells DU-145 and PC-3. (b,d) Their 4-ene-3-oxosteroids (DOC and progesterone) had also some ability to stimulate cell proliferation. Prostate cancer (PC) cells were treated with the indicated concentration of each steroid (x-axis, 10⁻¹⁰–10⁻⁶ M) and 72 h later, MTT (3-[4,5-dimethylthiazol-2-yl]-2,5-diphenyltetrazolium bromide) assay was performed. Y-axis: absorbance (ABS) at 490 nm (MTT assay), and at 630 nm as a reference, measured with a microplate reader. Each assay was tested six times and the means \pm SD were plotted.

AR by each of the steroids. As shown in Figure 2(a), both 5 α DH-DOC and DOC at 10⁻⁷ M or lower concentration showed some level of AR transactivation in LNCaP cells (mutant AR: T877A) and 22Rv1 cells (mutant AR: H874Y). 5 α -Dihydro-deoxycorticosterone (5 α DH-DOC) and DOC treatment showed transactivation of wild-type AR (Fig. 2b, left) and mutant AR (Fig. 2b, right) which was introduced in AR-null PC-3 cells, although they did not show any transactivation activity in mock-transfected PC-3 cells (Fig. 2b, lower). These transactivation activities were blocked by the AR antagonist bicalutamide (BCL), confirming that they were caused via AR, regardless of its mutation status. Interestingly, 5 α DH-DOC showed more impact on the transactivation activity of wild-type AR than DOC (Fig. 2b, left), while 5 α DH-DOC did not show any advantageous impact on the transactivation activity of mutant AR (T877S) over DOC (Fig. 2b, right). This was consistent with the findings that 5 α DH-DOC showed less effect on the transactivation of mutant ARs in LNCaP cells and 22Rv1 cells than DOC. On the other hand, 5 α DH-progesterone and other 5 α DH-oxosteroids did not show such a characteristic feature to induce AR transactivation (Fig. 2c,d for 5 α DH-progesterone, and data are not shown as for other 5 α DH-steroids), except for DHT. These findings suggest that the conversion from DOC to

5 α DH-DOC by 5 α -steroid reductases could provide some advantageous effects on AR transactivation to PC cells with wild-type AR, as well as the conversion from testosterone to DHT. Most of CRPC cells showed overexpression of wild-type AR, not mutant AR,⁽¹³⁾ and these effects of 5 α DH-DOC on wild-type AR might be beneficial for CRPC cells. Thus we focused on 5 α DH-DOC and DOC in further experiments.

Type 1 5 α -steroid reductase (SRD5A1) was responsible for 5 α DH-DOC production in PC cells. In PC tissues, especially CRPC tissues, type 1 (SRD5A1) and type 3 (SRD5A3) isozymes are up-regulated and dominant^(11,14) and also their expressions were observed in all available PC cell lines (Fig. S2). They are likely to be responsible for DHT and other 5 α DH-steroid production in PC tissues. To investigate which of type 1 and/or type 3 is responsible for 5 α DH-DOC production in PC cells, COS7 cells were transfected with each of HA-tagged expression vectors (SRD5A1, SRD5A3, and mock, Fig. 3a) and the cells were treated with 10⁻⁶ M DOC. One hour after incubation under 10⁻⁶ M DOC, the conditioned media were harvested to measure the amounts of 5 α DH-DOC by sensitive LC-MS/MS analysis. As a result, a much higher amount of 5 α DH-DOC was observed in the cells that overexpressed SRD5A1 than in the SRD5A3 or mock-transfected (Fig. 3b) cells. The production of 5 α DH-DOC

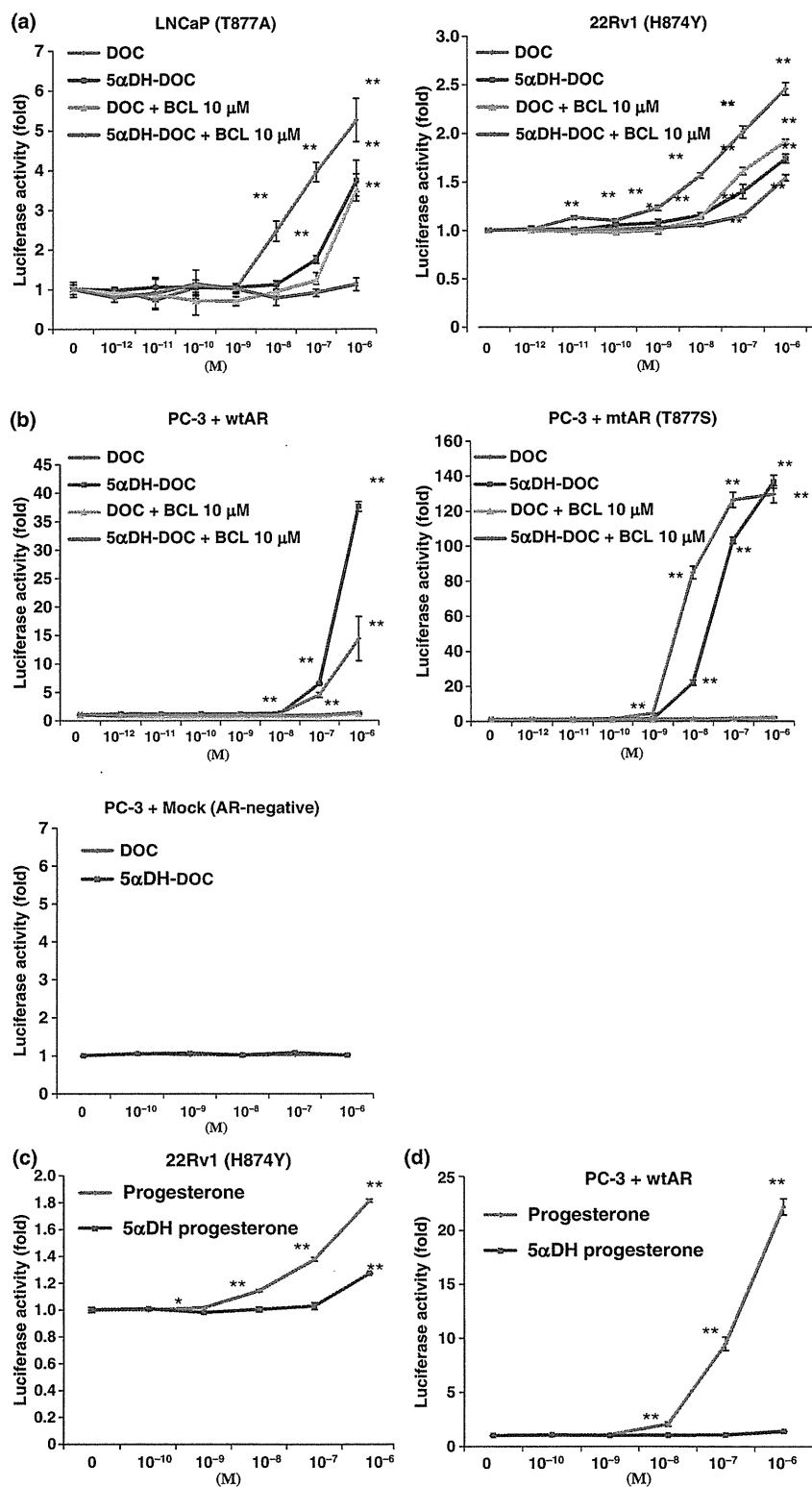


Fig. 2. Luciferase assays of 5αDH steroids and their precursors for androgen receptor (AR) transactivation activity. (a) LNCaP cells and 22Rv1 cells were transfected with pGL3-PSA and the luciferase activity in the presence of indicated concentration (x-axis) of 5α-dihydro-deoxycorticosterone (5αDH-DOC) and 11-deoxycorticosterone (DOC) was compared. LNCaP cells and 22Rv1 cells expressed mutant AR, T877A, and H874Y, respectively. (b) Androgen receptor (AR)-null PC-3 cells were co-transfected with wild-type AR (left), mutant AR-T877A (right), or mock (lower) and pGL3-PSA and the luciferase activity in the presence of indicated concentration (x-axis) of 5αDH-DOC and DOC was compared. These luciferase activities were blocked by antiandrogen bicalutamide (BCL). Each assay was tested six times and the means ± SD were plotted. **P* < 0.05, ***P* < 0.01 by Student's *t*-test. (c) 22Rv1 cells were transfected with pGL3-PSA and the luciferase activity in the presence of indicated concentration (x-axis) of 5αDH-progesterone and progesterone was compared. (d) Androgen receptor (AR)-null PC-3 cells were co-transfected with wild-type AR and pGL3-PSA and the luciferase activity in the presence of indicated concentration (x-axis) of 5αDH-progesterone and progesterone was compared. Each assay was tested six times and the means ± SD were plotted. **P* < 0.05, ***P* < 0.01 by Student's *t*-test.

was inhibited by pre-treatment of 1 μM dutasteride which could inhibit the activity of SRD5A1 (Fig. 3c). These findings indicated that SRD5A1 could be responsible for 5αDH-DOC production *in vitro*.

Subsequently, to evaluate the endogenous activity of SRD5A1 for 5αDH-DOC, 22Rv1 cells were treated with siRNA duplex specific to *SRD5A1* (siSRD5A1) or the control siRNA duplex (siEGFP). Reverse transcription (RT)-PCR validated the knockdown

effect by siSRD5A1 (Fig. 4a), and siSRD5A1 treatment suppressed the cell viability of 22Rv1 cells, compared with the control siEGFP (Fig. 4b, *P* < 0.01). The amount of 5αDH-DOC production was also significantly decreased in the conditioned media of 22Rv1 of which *SRD5A1* was knocked down (Fig. 4c, *P* < 0.01). These findings suggest that SRD5A1 is likely to play some important roles in converting DOC to 5αDH-DOC in PC cells, as well as PC cell viability.

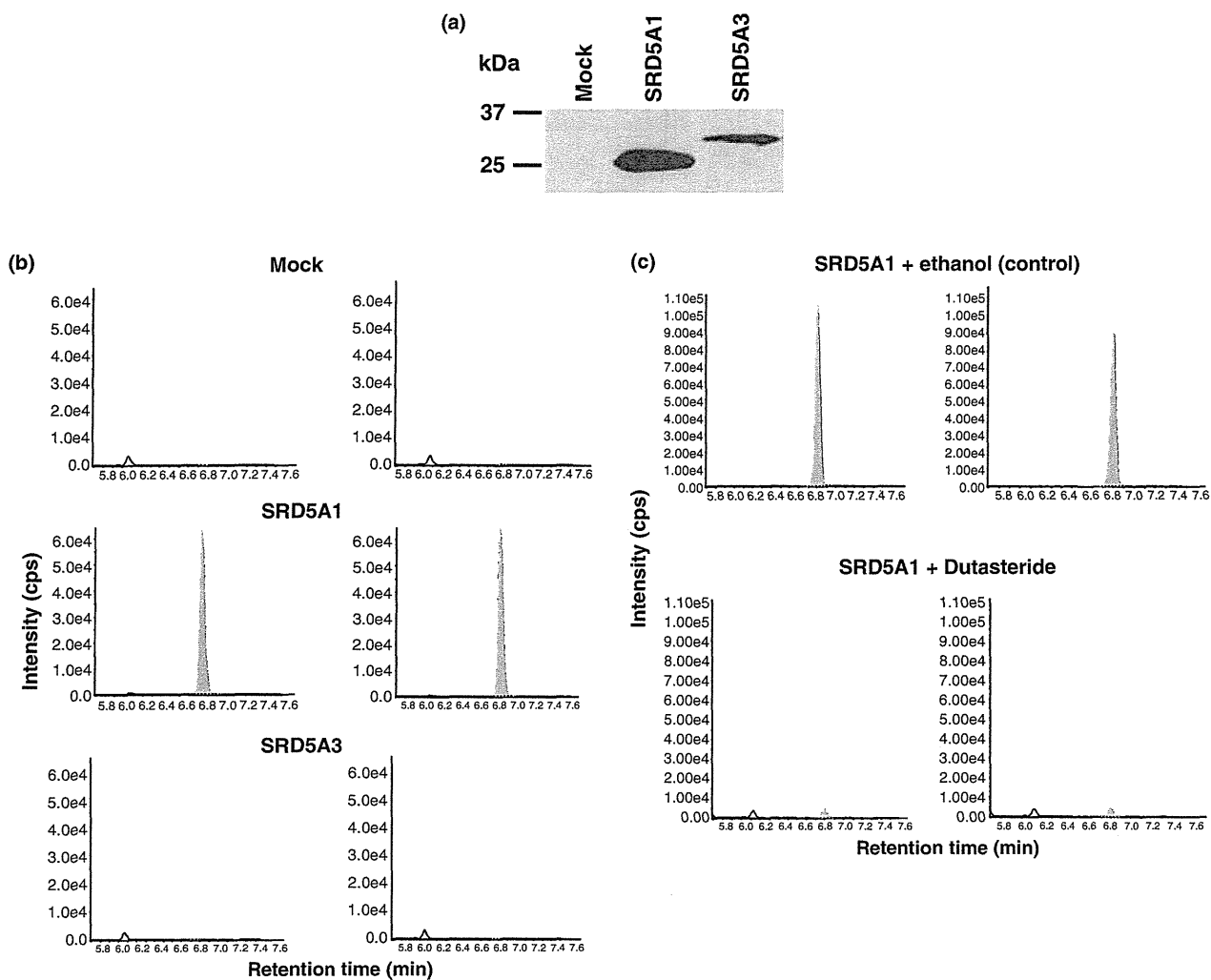


Fig. 3. Type 1 5 α -steroid reductase (SRD5A1) was responsible for the production of 5 α -dihydro-deoxycorticosterone (5 α DH-DOC). (a) COS7 cells were transfected with SRD5A1, SRD5A3, or mock vector and the expression of exogenous SRD5A1 and SRD5A3 were evaluated by western blot analysis using anti-HA tag antibody. (b) The transfected cells were treated with 10⁻⁶ M 11-deoxycorticosterone (DOC), and after 1 h of incubation, the conditioned media were harvested. Liquid chromatography-tandem mass spectrometry (LC-MS/MS) analysis of the media specifically detected the production of 5 α DH-DOC which was converted from DOC in COS7 cells overexpressing SRD5A1 (middle panel), but not in COS7 cells overexpressing SRD5A3 (lower panel) or mock cells (upper panel). These experiments were performed in duplicate (right and left panels). (c) 1- μ M Dutasteride treatment inhibited 5 α DH-DOC production in COS7 cells transfected with SRD5A1 vector. 5 α -Dihydro-deoxycorticosterone (5 α DH-DOC) was detected by LC-MS/MS and these experiments were performed in duplicate (right and left panels).

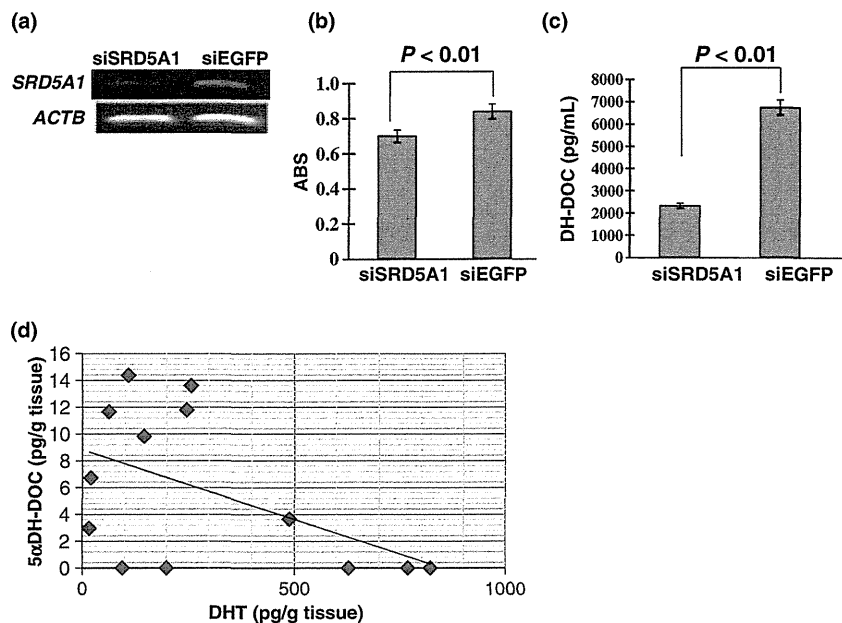
5 α -Dihydro-deoxycorticosterone (5 α DH-DOC) was detected in clinical CRPC tissues by LC-MS/MS. To prove the presence of 5 α DH-DOC in clinical CRPC tissues, we extracted steroid fractions from 13 fresh frozen CRPC tissues and measured the intratumoral 5 α DH-DOC and DHT levels by the sensitive LC-MS/MS analysis we established here. As expected, the intratumoral DHT level in all CRPC samples was below 1000 pg/g tissues, and 5 α DH-DOC was detected in eight out of 13 CRPC tissues (Fig. 4d). We did not find any clinical features of these 5 α DH-DOC-positive CRPCs. Interestingly, 5 α DH-DOC-positive CRPCs had a comparatively lower level of DHT, and the level of 5 α DH-DOC was significantly inversely correlated to the DHT level within CRPC tissues (Pearson $r = -0.5727$, $P < 0.05$).

Discussion

Several molecular events that drive the progression to the castration-resistant state have been proposed and extensively

reviewed.^(5,6,15-17) One of the key and main mechanisms is overexpression of wild-type AR with or without amplification of the AR gene, which is commonly observed in clinical CRPCs.^(6,12,18,19) On the other hand, AR mutations allow AR activation by low androgen levels or by other endogenous steroids such as corticosteroids and antiandrogens,⁽²⁰⁻²³⁾ but the incidence of AR mutation is <20% in clinical CRPCs.⁽¹³⁾ In this study, we searched for novel 5 α DH steroids that could have any potential to stimulate PC cell growth as well as AR activity, and among them, we here focused on 5 α DH-DOC and demonstrated that it could stimulate wild-type AR preferentially rather than mutant AR, and type 1 5 α -steroid reductase overexpressed in CRPC cells could be responsible for 5 α DH-DOC production. These findings indicate that 5 α DH-DOC and other unknown products of 5 α -steroid reductases (type 1 and type 3) could activate AR under extremely low levels of DHT in some CRPC cases and provide some survival advantages to PC cells, although the concentration of 5 α DH-DOC we here showed was relatively lower than that of DHT. *In situ* steroidogenesis

Fig. 4. (a) Reverse transcription (RT)-PCR confirmed knockdown effect on type 1 5 α -steroid reductase (*SRD5A1*) expression by siSRD5A1 in 22Rv1 cells. β -Actin (*ACTB*) was used to quantify the input RNAs. (b) Knockdown of *SRD5A1* expression by siSRD5A1 suppressed the proliferation of 22Rv1 cells, compared with the control RNA duplex siEGFP ($P < 0.01$, Student's *t*-test). Y-axis, absorbance (ABS) at 490 nm (MTT assay), and at 630 nm as a reference, measured with a microplate reader. (c) Suppression of *SRD5A1* expression by siSRD5A1 reduced 5 α -dihydro-deoxycorticosterone (5 α DH-DOC) production in 22Rv1 cells ($P < 0.01$, Student's *t*-test). 5 α -Dihydro-deoxycorticosterone (5 α DH-DOC) in the media was measured by liquid chromatography-tandem mass spectrometry (LC-MS/MS) analysis. (d) Detection of 5 α DH-DOC and DHT in 13 clinical CRPC tissues. 5 α -Dihydro-deoxycorticosterone (5 α DH-DOC) was detected by sensitive LC-MS/MS in clinical CRPC tissues. 5 α -Dihydrotestosterone (DHT) was also measured by sensitive LC-MS/MS in the same tissues, and the level of 5 α DH-DOC was inversely correlated with the low level of DHT concentration (Pearson $r = -0.5727$, $P < 0.05$).



including this 5 α -steroid reduction is likely to be one of the key mechanisms of CRPC development and a good molecular target for CRPC treatment.

In the standard steroidogenesis pathway, the testes provide the major source of androgens, particularly testosterone. Alternatively, prostate cells can convert adrenal-derived steroids, such as androstenediol and DHEA (dehydroepiandrosterone), to testosterone by 17 β -hydroxysteroid dehydrogenase and 3 β -hydroxysteroid dehydrogenase.^(17,24) Currently, there is increasing evidence that PC cells can synthesize androgens *de novo* instead of receiving them through the bloodstream.^(17,25) This concept is supported by the fact that expressions of several enzymes responsible for steroid synthesis were up-regulated in CRPCs^(26–28) and they are likely to play some critical roles in the CRPC phenotype. Among them, cytochrome P17 (CYP17) catalyzes the key reactions to androgen and estrogen biosynthesis, and its selective inhibitor, abiraterone, is now in clinical trials for CRPCs, showing significant antitumor activity in CRPCs,⁽²⁹⁾ indicating that CRPCs remain dependent on ligand-activated AR signaling, and also these findings suggest that such steroids or androgen metabolism enzymes could be potential molecular therapeutic targets for CRPCs. Among several steroid metabolism enzymes altered in CRPCs, 5 α -steroid reductases mostly contribute to both the standard steroidogenesis pathway (testosterone to DHT), and the alternative steroidogenesis pathway which is likely to be activated when testosterone are not available from the blood circulation.^(16,24) In addition to DHT, other various types of steroids can be subject to the reduction of 5 α -steroid reductases to acquire more potentials as functional steroids or modify/change their functions.⁽³⁰⁾ Neuroendocrine cells in the brain highly express type 1 5 α -steroid reductase (*SRD5A1*) and produce several neurosteroids such as 5 α DH-progesterone, allopregnanolone (ALLO), and tetrahydrodeoxycorticosterone

(THDOC), which modulate GABA action at GABA_A receptors to contribute to neuroendocrine transmission.⁽³¹⁾ In this point, 5 α DH-DOC production by *SRD5A1* in CRPCs may reflect the neuroendocrine-like phenotype of CRPCs,^(32,33) and in addition to AR activation, it may regulate or stimulate other signaling pathways similar to how other 5 α DH neurosteroids to contribute to the CRPC phenotype.

The source of DHT in prostatic tissue after ADT is likely to be intracrine production within the prostate, which converts adrenal androgens to DHT.⁽⁹⁾ Interestingly, we observed that the level of 5 α DH-DOC was significantly inversely correlated to the DHT level within CRPC tissues, although the concentration of 5 α DH-DOC was quite lower than that of DHT. This might implicate that when DHT levels were declined within CRPC tissues, there might still be compensatory increases in 5 α DH-DOC and other unknown 5 α DH steroids to activate AR by taking advantage of overexpressing *SRD5A1* or *SRD5A3*. There is no evidence obtained so far by clinical trials to support the sole treatment with dutasteride; dual inhibitor of type 1 and 2 5 α -steroid reductases could effectively suppress CRPC growth, although the DHT level within PC tissues was not assessed.^(34,35) Several other ligands can activate the AR pathway or other pathways to support the survival of PC cells under the castrated and 5 α -steroid reductase-free environment, and the combination hormonal or AR-targeting therapy with dutasteride might be required to deplete intratumoral active steroids in CRPCs and suppress CRPC growth effectively.

Acknowledgments

We thank Ms U. Mami for her technical assistance. This work was supported in part by research grants (#18590323 to H. Nakagawa) and (#00L01402 to Y. Nakamura) from the Japan Society for the Promotion of Science.

References

- Gronberg H. Prostate cancer epidemiology. *Lancet* 2003; **361**: 859–64.
- Smaletz O, Scher HI. Outcome predictions for patients with metastatic prostate cancer. *Semin Urol Oncol* 2002; **20**: 155–63.
- Petrylak DP, Tangen CM, Hussain MHA *et al*. Docetaxel and estramustine compared with mitoxantrone and prednisone for advanced refractory prostate cancer. *N Engl J Med* 2004; **351**: 1513–20.

- Tannock IF, de Wit R, Berry WR *et al*. Docetaxel plus prednisone or mitoxantrone plus prednisone for advanced prostate cancer. *N Engl J Med* 2004; **351**: 1502–12.
- Scher HI, Sawyers CL. Biology of progressive, castration-resistant prostate cancer: directed therapies targeting the androgen-receptor signaling axis. *J Clin Oncol* 2005; **23**: 8253–61.
- Chen Y, Sawyers CL, Scher HI. Targeting the androgen receptor pathway in prostate cancer. *Curr Opin Pharmacol* 2008; **8**: 440–8.

- 7 Thigpen AE, Silver RI, Guileyardo JM, Casey ML, McConnell JD, Russell DW. Tissue distribution and ontogeny of steroid 5 alpha-reductase isozyme expression. *J Clin Invest* 1993; **92**: 903–10.
- 8 Mohler JL, Gregory CW, Ford OH *et al.* The androgen axis in recurrent prostate cancer. *Clin Cancer Res* 2004; **10**: 440–8.
- 9 Nishiyama T, Hashimoto Y, Takahashi K. The influence of androgen deprivation therapy on dihydrotestosterone levels in the prostatic tissue of patients with prostate cancer. *Clin Cancer Res* 2004; **10**: 7121–6.
- 10 Titus MA, Schell MJ, Lih FB, Tomer KB, Mohler JL. Testosterone and dihydrotestosterone tissue levels in recurrent prostate cancer. *Clin Cancer Res* 2005; **11**: 4653–7.
- 11 Uemura M, Tamura K, Chung S *et al.* Novel 5 α -steroid reductase (SRD5A3, type-3) is overexpressed in hormone-refractory prostate cancer. *Cancer Sci* 2008; **99**: 81–6.
- 12 Tamura K, Furihata M, Tsunoda T *et al.* Molecular features of hormone-refractory prostate cancer cells by genome-wide gene expression profiles. *Cancer Res* 2007; **67**: 5117–25.
- 13 Taplin M-E, Rajeshkumar B, Halabi S *et al.* Androgen receptor mutations in androgen-independent prostate cancer: Cancer and Leukemia Group B Study 9663. *J Clin Oncol* 2003; **21**: 2673–8.
- 14 Titus MA, Gregory CW, Ford OH, Schell MJ, Maygarden SJ, Mohler JL. Steroid 5 α -reductase isozymes I and II in recurrent prostate cancer. *Clin Cancer Res* 2005; **11**: 4365–71.
- 15 Feldman BJ, Feldman D. The development of androgen-independent prostate cancer. *Nat Rev Cancer* 2001; **1**: 34–45.
- 16 Vis AN, Schroder FH. Key targets of hormonal treatment of prostate cancer. Part I: the androgen receptor and steroidogenic pathways. *BJU Int* 2009; **104**: 438–48.
- 17 Attar RM, Takimoto CH, Gottardis MM. Castration-resistant prostate cancer: locking up the molecular escape routes. *Clin Cancer Res* 2009; **15**: 3251–5.
- 18 Linja MJ, Savinainen KJ, Saramaki OR, Tammela TLJ, Vessella RL, Visakorpi T. Amplification and overexpression of androgen receptor gene in hormone-refractory prostate cancer. *Cancer Res* 2001; **61**: 3550–5.
- 19 Ford OH, Gregory CW, Kim D, Smitherman AB, Mohler JL. Androgen receptor gene amplification and protein expression in recurrent prostate cancer. *J Urol* 2003; **170**: 1817–21.
- 20 Culig Z, Hobisch A, Cronauer MV *et al.* Mutant androgen receptor detected in an advanced-stage prostatic carcinoma is activated by adrenal androgens and progesterone. *Mol Endocrinol* 1993; **7**: 1541–50.
- 21 Taplin M-E, Bubley GJ, Shuster TD *et al.* Mutation of the androgen-receptor gene in metastatic androgen-independent prostate cancer. *N Engl J Med* 1995; **332**: 1393–8.
- 22 Zhao XY, Malloy PJ, Krishnan AV *et al.* Glucocorticoids can promote androgen-independent growth of prostate cancer cells through a mutated androgen receptor. *Nat Med* 2000; **6**: 703–6.
- 23 Mizokami A, Koh E, Fujita H *et al.* The adrenal androgen androstenediol is present in prostate cancer tissue after androgen deprivation therapy and activates mutated androgen receptor. *Cancer Res* 2004; **64**: 765–71.
- 24 Ghayee HK, Auchus RJ. Clinical implications of androgen synthesis via 5 α -reduced precursors. *Endocr Dev* 2008; **13**: 55–66.
- 25 Attard G, Reid AHM, Olmos D, de Bono JS. Antitumor activity with CYP17 blockade indicates that castration-resistant prostate cancer frequently remains hormone driven. *Cancer Res* 2009; **69**: 4937–40.
- 26 Stanbrough M, Bubley GJ, Ross K *et al.* Increased expression of genes converting adrenal androgens to testosterone in androgen-independent prostate cancer. *Cancer Res* 2006; **66**: 2815–25.
- 27 Locke JA, Guns ES, Lubik AA *et al.* Androgen levels increase by intratumoral de novo steroidogenesis during progression of castration-resistant prostate cancer. *Cancer Res* 2008; **68**: 6407–15.
- 28 Montgomery RB, Mostaghel EA, Vessella R *et al.* Maintenance of intratumoral androgens in metastatic prostate cancer: a mechanism for castration-resistant tumor growth. *Cancer Res* 2008; **68**: 4447–54.
- 29 Attard G, Reid AHM, Yap TA *et al.* Phase I clinical trial of a selective inhibitor of CYP17, abiraterone acetate, confirms that castration-resistant prostate cancer commonly remains hormone driven. *J Clin Oncol* 2008; **26**: 4563–71.
- 30 Wilson JD. The role of 5 α -reduction in steroid hormone physiology. *Reprod Fertil Dev* 2001; **13**: 673–8.
- 31 Agis-Balboa RC, Pinna G, Zhubi A *et al.* Characterization of brain neurons that express enzymes mediating neurosteroid biosynthesis. *Proc Natl Acad Sci USA* 2006; **103**: 14602–7.
- 32 Hirano D, Okada Y, Minei S, Takimoto Y, Nemoto N. Neuroendocrine differentiation in hormone refractory prostate cancer following androgen deprivation therapy. *Eur Urol* 2004; **45**: 586–92.
- 33 Yuan T-C, Veeramani S, Lin M-F. Neuroendocrine-like prostate cancer cells: neuroendocrine transdifferentiation of prostate adenocarcinoma cells. *Endocr Relat Cancer* 2007; **14**: 531–47.
- 34 Shah SK, Trump DL, Sartor O, Tan W, Wilding GE, Mohler JL. Phase II study of dutasteride for recurrent prostate cancer during androgen deprivation therapy. *J Urol* 2009; **181**: 621–6.
- 35 Taplin M-E, Regan MM, Ko Y-J *et al.* Phase II study of androgen synthesis inhibition with ketoconazole, hydrocortisone, and dutasteride in asymptomatic castration-resistant prostate cancer. *Clin Cancer Res* 2009; **15**: 7099–105.

Supporting Information

Additional Supporting Information may be found in the online version of this article:

Fig. S1. Cell growth assays of 5 α DH steroids and their precursors. Corticosterone (a) and cortisol (c) had positive effect on the proliferation of androgen receptor (AR)-negative DU-145 cells, as well as LNCaP or 22RV1 cells. 5 α DH-Corticosterone (b) and 5 α DH-cortisol (d) did not show any significant growth-promoting effect on prostate cancer (PC) cell lines. Prostate cancer (PC) cells were treated with indicated concentration of each steroid (x -axis, 10^{-10} – 10^{-6} M) and 72 h later, MTT assay was performed. Y -axis: absorbance (ABS) at 490 nm (MTT assay), and at 630 nm as a reference, measured with a microplate reader. Each assay was tested six times and the means \pm SD. were plotted.

Fig. S2. Semi-quantitative RT-PCR showed that all of the prostate cancer (PC) cell lines we used expressed type 3 5 α -steroid reductase (SRD5A1) and *SRD5A1*. Expression of β -actin (*ACTB*) served as the quantitative control.

Please note: Wiley-Blackwell are not responsible for the content or functionality of any supporting materials supplied by the authors. Any queries (other than missing material) should be directed to the corresponding author for the article.

Forkhead box A1 transcriptional pathway in KRT7-expressing esophageal squamous cell carcinomas with extensive lymph node metastasis

MASAYUKI SANO^{1,5}, KAZUHIKO AOYAGI¹, HIRO TAKAHASHI^{4,5,7}, TAKESHI KAWAMURA⁷, TOMOKO MABUCHI¹, HIROYASU IGAKI², YUJI TACHIMORI², HOICHI KATO², ATSUSHI OCHIAI³, HIROYUKI HONDA⁷, YUJI NIMURA⁸, MASATO NAGINO⁶, TERUHIKO YOSHIDA¹ and HIROKI SASAKI¹

¹Genetics Division and ²Department of Surgery, National Cancer Center Research Institute and Central Hospital, Department of Surgery, 5-1-1 Tsukiji, Chuo-ku, Tokyo 104-0045; ³Pathology Division, Research Cancer for Innovative Oncology, National Cancer Center Hospital East, 6-3-1 Kashiwanoha, Kashiwa, Chiba 277-8577; ⁴College of Bioscience and Biotechnology, ⁵Plant Biology Research Center, Chubu University, Matsumoto-cho 1200, Kasugai, Aichi 487-8501; ⁶Division of Surgical Oncology, Department of Surgery, Nagoya University Graduate School of Medicine, Tsurumai, Showa-ku, ⁷Department of Biotechnology, Nagoya University Graduate School of Engineering, Furo-cho, Chikusa-ku, Nagoya 464-8603; ⁸Aichi Cancer Center, 1-1 Kakodono, Chikusa-ku, Nagoya 464-8681, Japan

Received September 7, 2009; Accepted October 18, 2009

DOI: 10.3892/ijo_00000503

Abstract. Prognosis of cancers with lymph node metastasis is known to be very poor; however, it is still controversial whether metastatic potential can be evaluated by expression profiles of primary tumors. Therefore, to address this issue, we compared gene expression profiles of 24 esophageal squamous cell carcinomas (ESCCs) with extensive lymph node metastasis and 11 ESCCs with no metastatic lymph node. However, there was no gene cluster distinguishing these two groups, suggesting that lymph node metastasis-associated genes are varied depending on cases or subgroups. Therefore, we applied a recently developed filtering method (S2N') to identify such genes, and successfully extracted 209 genes associated with node status. Among them, over-expression of *CALB1*, *KRT7/CK7*, *MUC1* and *CEA/CEACAM5* in poor prognostic cases with metastatic lymph nodes was confirmed in two sets of ESCCs by RT-PCR. Each often seemed to have glandular cell type-characteristics in both the gene expression and morphology. It was also revealed that *FOXA1* siRNA treatment of esophageal cancer cells reduced the mRNA level of both *KRT7* and a stabilizer of epithelial-mesenchymal transition (EMT) regulator *LOXL2*, and that both *FOXA1* and *LOXL2* siRNAs reduced invasion and

migration of ESCC cells. In 15 *KRT7*-expressing ESCCs with metastatic lymph nodes, 60% expressed *FOXA1* and 33% expressed both *FOXA1* and *LOXL2*. These results suggest that *FOXA1* induces not only *KRT7* but also *LOXL2* in a subset of poor prognostic ESCCs with metastatic lymph nodes, and it is also plausible, that other *FOXA1* downstream genes could be therapeutic targets of poor prognostic ESCCs.

Introduction

Cancer is a major cause of human deaths world-wide. Gene expression data from DNA microarrays are individualized and useful in the diagnosis and prognosis of diseases (1). Esophageal cancer is the eighth most common cancer and the sixth most common cause of cancer-related mortality (2). Esophageal cancer in East Asian countries and some parts of Europe consists mainly of squamous cell carcinomas. Chemoradiotherapy (CRT) followed by surgery is the standard therapy in Western countries. In Japan, CRT or neoadjuvant chemotherapy followed by surgery and definitive CRT are the standard therapies (3). For locally advanced esophageal cancers, surgery is still the standard therapy in Japan. A recent improvement in surgical resection following radical node dissection has been reported with 5-year survival rates of 31-55% (4). Yet also in this cancer, lymph node metastasis has been reported to be a most strong marker for poor prognosis in patients with the improved surgery (4), especially, those patients with >5 metastatic lymph nodes did very poorly compared with patients with no metastatic lymph nodes. Thus, lymph node metastasis is known to be tightly associated with a poor prognosis in many surgically resectable solid tumors. Identification of genes associated with lymph node metastasis is very important for

Correspondence to: Dr Hiroki Sasaki, Genetics Division, National Cancer Center Research Institute, 1-1, Tsukiji 5-chome, Chuo-ku, Tokyo 104-0045, Japan
E-mail: hksasaki@ncc.go.jp

Key words: microarray, FOXA1, KRT7/CK7, LOXL2, esophageal cancer

establishing a molecular diagnosis and also for understanding the malignant phenotype; however, it is still controversial whether metastatic potential can be evaluated by expression profiles of primary tumors. Esophageal cancer provides an opportunity to address such an important issue.

For a marker gene selection from mRNA expression profiles, the use of one of the many filtering methods is necessary, such as Mann-Whitney's U-test, Student's t-test, Welch's t-test, signal-to-noise (S2N) (5), significance analysis of microarrays (SAM) (6), and nearest shrunken centroids (NSC) (7). In our previous study, we developed the projective adaptive resonance theory (PART) filtering method (8) and reported that the PART filtering method showed a better performance than conventional methods such as S2N and NSC (9-14). By the PART method, the genes that have a low variance in the gene expression level in either of two classes or subgroups can be selected. We further developed another simple and practical filtering method, modified S2N (S2N) (12), based on the concept underlying the PART filtering method. The S2N' filtering method was statistically superior to the conventional methods such as Mann-Whitney's U-test, Student's t-test, Welch's t-test, S2N, SAM and NSC (12).

In the present study, we applied S2N' to genome-wide gene expression profiles to identify marker genes for poor prognostic esophageal squamous cell carcinomas (ESCCs) with lymph node metastasis, and successfully identified FOXA1 transcriptional pathways for cell invasion or migration in a subset of such ESCCs.

Materials and methods

Tissue samples. All cases of esophageal cancers examined in this study were diagnosed as squamous cell carcinoma. All esophageal squamous cell carcinoma (ESCC) patients underwent surgical resection following two- or three-field node dissection between 1994 and 2000 at the Central Hospital of the National Cancer Center. ESCC tissues were provided after obtaining informed consent from each patient and approval by the Center's Ethics Committee.

Microarray analysis. Gene expression profile data were obtained from 35 surgical specimens from ESCC patients: 24 patients with >5 metastatic lymph nodes (N5 group) and 11 patients with no metastatic lymph node (N0 group). For RNA extraction, trained pathologists carefully excised bulk tissue samples from the main tumor, leaving a clear margin from the surrounding normal tissue. Total RNAs extracted from the bulk tissue samples were biotin-labeled and hybridized to high-density oligonucleotide microarrays (Human Expression Array U95A version 2, Affymetrix, Santa Clara, CA, USA) according to the manufacturer's instructions. The scanned data of the arrays were processed by GeneChip Analysis Suite version 4.0, which scaled the average intensity of all the genes on each array to a target signal of 1,000 to reliably compare variable multiple arrays.

S2N' filtering of gene expression profiles. The S2N' filtering method for gene selection from microarray data was originally developed by us (12). This method allows us to extract

as a marker gene even in the case that only a single gene (or a few genes) was expressed specifically in one of the two groups. By this method, we selected the top 209 marker gene candidates which were expressed preferentially in one of the two groups (N0 and N5) in this study.

Survival analysis and hierarchical clustering analysis. The Kaplan-Meier metastases analysis plots were formulated using WinSTAT Statistics for Windows ver. 3.1 (Light Stone, Tokyo, Japan). The significance of the difference in survival rates was analyzed using a log-rank test (Mantel-Cox method). Hierarchical clustering is widely used as one of the unsupervised learning methods. In this study, hierarchical clustering of microarray data of 35 ESCCs was performed by the use of CLUSTER software (15).

Semi-quantitative and quantitative RT-PCR. Surgical specimens were snap-frozen in liquid nitrogen. Total RNA was isolated by suspending the cells in Isogen lysis buffer (Nippon Gene, Toyama, Japan) followed by precipitation with isopropanol. RT-PCR was carried out using primer sets designed for detecting the 3' side of cDNA of each gene: for *CALB1*, 5'-AATCAAAATGTGTGGGAAAG-3' and 5'-CCCAGCACGAGAATAAGAG-3', for *TFE3*, 5'-CTGAGGCACCTCCAGCTGCCCCG-3' and 5'-GGAGCATGGGACCTTTTCG-3', for *KRT7*, 5'-CTGAAGGCTTATTCCATCCG-3' and 5'-CCTCAGAATGAGGCTGCTTT-3', for *CLDN10*, 5'-ACGGCTAACTGGATAACTGA-3' and 5'-TGTCTCACTCACTCCTACA-3', for *MUC1*, 5'-AATTGACTCTGGCCTTCCGA-3' and 5'-GCCACCATTACCTGCAGAAA-3', for *CEA*, 5'-AGACTCTGACCAGAGATCGA-3' and 5'-GGTGGACAGTTTCATGAAGC-3', for *PGC*, 5'-CCAGCTTGACCTTCATCATC-3' and 5'-GCTGAATCCAGAGTGGAAG-3', for *LIPF*, 5'-ACGAGTCGCTTGGATGTGA-3' and 5'-CGTTCACACTGCAATTGGT-3', for *LOXL2*, 5'-CACCATGTGTCATCACAGAC-3' and 5'-CTCCTTAGATTGCTTCTCC-3', for *FOXA1*, 5'-GGTCATGTCAATTCTGAGGTC-3' and 5'-TAACACCATGTCCAACCTGTG-3', for *ACTB* (β -actin), 5'-TCATCACCATTGGCAATGAG-3' and 5'-CAC TGTGTTGGCGTACAGGT-3'.

For semi-quantitative RT-PCR, we showed data within linear range by performing 25-35 cycles of PCR. Quantitative real-time PCR was performed by a Bio-Rad iCycler with iQ Syber Green Supermix (Bio-Rad, Hercules, CA, USA) as directed by the manufacturer. The value of $1/2^N$ (N : the number of PCR cycles corresponding to the onset of the linear amplification of each gene product) was calculated as a relative mRNA expression level of each gene normalized to *ACTB*. The data from 2 independent analyses for each sample were averaged.

Immunohistochemistry. All resected specimens were fixed in either 10% formalin or methanol and embedded in paraffin. Tissue sections of 4 μ m in thickness were cut from a paraffin-embedded block including the most representative area of the tumor, and were used for immunohistochemical staining. The sections were deparaffinized in xylene, dehydrated in a graded series of ethanol, and immersed in methanol with 0.3% hydrogen peroxide for 15 min to inhibit endogenous peroxidase activity. The slides were heated at 95°C for 20 min

in a microwave oven in a citrate buffer with pH 6.0 for antigen retrieval, and allowed to cool to room temperature. Non-specific binding was blocked by preincubation with 2% normal swine serum in phosphate-buffered saline (PBS) for 60 min at room temperature. The slides were then incubated overnight at 4°C with respective primary antibodies. The slides were washed three times with PBS and incubated with EnVision (Dako, Carpinteria, CA, USA) for 1 h at room temperature. The sections were visualized using 3, 3'-diaminobenzidine tetrahydrochloride in 50 mM Tris-buffer (pH 7.6) containing 0.3% hydrogen peroxide as the chromogen, and counterstained by hematoxylin. Antibodies used in this study were anti-CK7 (mouse monoclonal, clone OV-TL, Dako, 1:50).

siRNA transfection. The esophageal cancer cell line TE3 was used in this study because among 6 cell lines (TE1, TE3, TE5, TE6, TE8 and TE10), TE3 has been reported to maintain the expression profile of primary esophageal cancers and to most mimick the basal cell (12). Three or four small interfering (si)RNA fragments were used for suppressing *FOXA1*, *KRT7* and *LOXL2* mRNA expression respectively, and the most effective one was selected by quantitative real-time RT-PCR analysis; for *FOXA1* mRNA target sequence: 5'-GGAGAGATAAGTTATAGGG-3' (siRNA ID: 107428, Ambion, Austin, TX, USA); for *KRT7*: 5'-GGCTGAGATC GACAACAT-3' (siRNA ID: 215171, Ambion); for *LOXL2*: 5'-CCCTCCAGTCTATTATAGT-3' (siRNA ID: 114218, Ambion). The siRNAs including control siRNA (1022076, Qiagen, Valencia, CA, USA) were introduced to TE3 using DharmaFECT (Dharmacon, La Fayette, CO, USA) following the procedure recommended by the manufacturer. The RT-PCR and Matrigel invasion assay were carried out after siRNA treatment of TE3 cells.

Matrigel invasion and wound healing assays. Invasion of the esophageal cancer TE3 cells *in vitro* was measured by BD BioCoat™ Matrigel Invasion Chamber (BD Biosciences, San Jose, CA, USA) according to the manufacturer's protocol. After siRNA transfection, the cells were trypsinized and transferred into triplicate wells. After 24-h incubation, the cells that passed through the filter into the lower wells were fixed, stained and counted. For the wound healing assay, TE3 cells were grown till they were 90% confluent. A lineal scratch wound was made on the plate by a plastic tip. Images were taken every 12 h for 2 days.

Results

Survival analysis. The Kaplan-Meier method was performed on two groups: the N0 group consisting of 11 esophageal squamous cell carcinoma (ESCC) patients with no metastatic lymph node and the N5 group consisting of 24 ESCC patients with more than 5 metastatic lymph nodes. All patients underwent surgical resection following two- or three-field node dissection. These two groups showed a significant difference ($p < 0.001$) in survival rates after surgical resection (Fig. 1).

Calculation of S2N' values and ranking of each gene probe. First, we obtained mRNA expression profiles of ESCC

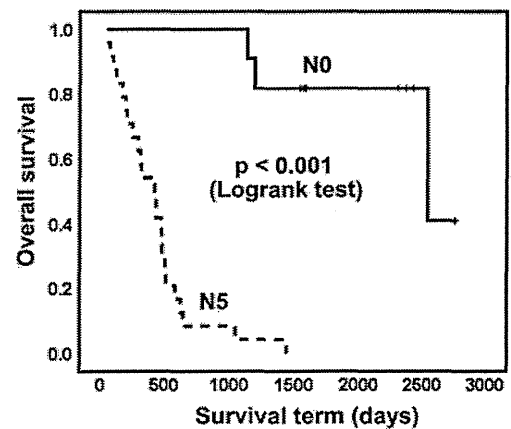


Figure 1. The Kaplan-Meier curve for each group. The N0 group with no metastatic lymph node consisted of 11 patients, and the N5 group with >5 metastatic lymph nodes consisted of 24 patients. The p-value was calculated by log-rank test.

tissues from a total of 35 patients of the two groups (N0 and N5). By unsupervised hierarchical clustering using various types of data processing, the two groups were not separated clearly (data not shown). These results implied that no large gene clusters associated with each group were present or that subgroups were present in each group. In this situation, the conventional filtering methods, such as Mann-Whitney's U-test, Student's t-test and Welch's t-test, were thought to be ineffective. In fact, only a few marker genes were selected by these t- or u-test methods (data not shown). The number of selected gene was too small to show significance. Therefore, we applied our previously developed S2N' method for marker gene selection in the two groups of ESCCs. The S2N' values were calculated for each gene probe and we successfully extracted 209 genes which were expressed preferentially in one of two groups. The top 50 genes were shown in Table I. However, this method allows us to extract a marker gene even in the case that only a single gene was expressed specifically in one of the two groups (12). Therefore, we have to further select genes with regards to the frequency of specific expression in one of the two groups. Of the top 50 genes, we selected 8 genes (Rank 1: *CALB1*; Rank 2: *TFF3*; Rank 3: *KRT7*; Rank 9: *CLDN10*; Rank 13: *FOXA1*; Rank 15: *MAL*; Rank 20: *CEACAM5*, and Rank 21: *MUC1*) that were found to be expressed preferentially and frequently in the N5 group. Their signal levels are shown in Fig. 2. These results suggest that our S2N' is very useful as a new method of candidate gene selection for genome-wide gene expression profiles obtained from microarrays.

RT-PCR analysis of 6 candidate marker genes in two sets of ESCCs with more than 5 metastatic lymph nodes or with no metastatic lymph node. Of the 8 genes, 6 (*CALB1*, *TFF3*, *KRT7/CK7*, *CLDN10*, *MUC1* and *CEA/CEACAM5*) were first analyzed by semi-quantitative RT-PCR in two independent sets of ESCCs: in the first set are 42 samples (12 patients with no metastatic lymph node including 11 N0 patients, and 30 patients with more than 5 metastatic lymph nodes including 24 N5 patients); in the second set are 22 samples

Table I. The top 50 marker gene candidates for the N0 or N5 group selected by the S2N¹ filtering method.

Probe set ID	GenBank accession	Gene symbol	S2N ¹ rank	S2N ¹	Marker type
36570_at	AF068862	CALB1	1	14.6	N5
31477_at	L08044	TFF3	2	8.2	N5
41294_at	AJ238246	KRT7	3	6.3	N5
39220_at	T92248	SCGB1A1	4	5.1	N5
38430_at	AA128249	FABP4	5	4.9	N0
174_s_at	U61167	ITSN2	6	4.5	N5
37149_s_at	U95626	LOC728320 /// LTF	7	4.3	N5
34637_f_at	M12963	ADH1A	8	4.0	N5
39579_at	U89916	CLDN10	9	3.7	N5
1497_at	L04270	LTBR	10	2.9	N0
38173_at	AB028999	SETD1B	11	2.7	N5
40193_at	X51956	ENO2	12	2.7	N0
37141_at	U39840	FOXA1	13	2.6	N5
35314_at	D63880	NCAPD2	14	2.6	N0
38051_at	X76220	MAL	15	2.5	N5
34873_at	Y16241	NEBL	16	2.5	N5
1890_at	AB000584	GDF15	17	2.3	N5
38648_at	U80760	ZNF384	18	2.3	N0
1389_at	J03779	MME	19	2.2	N5
1582_at	M29540	CEACAM5	20	2.1	N5
38784_g_at	J05581	MUC1	21	2.1	N5
41308_at	U37408	CTBP1	22	2.0	N5
37576_at	U52969	PCP4	23	2.0	N5
37687_i_at	M31932	FCGR2A	24	1.9	N5
1006_at	X07820	MMP10	25	1.9	N5
37242_at	U79260	FTO	26	1.9	N0
36123_at	D87292	TST	27	1.9	N5
1105_s_at	M12886	TRBV3-1 /// TRBV5-4 /// TRBV7-2	28	1.9	N5
1096_g_at	M28170	CD19	29	1.9	N5
36280_at	U26174	GZMK	30	1.9	N5
35425_at	AJ243512	BARX2	31	1.8	N5
37405_at	U29091	SELENBP1	32	1.8	N5
35227_at	U72066	RBBP8	33	1.7	N5
239_at	M63138	CTSD	34	1.7	N5
39249_at	AB001325	AQP3	35	1.7	N5
1020_s_at	U85611	CIB1	36	1.7	N5
41814_at	M29877	FUCA1	37	1.7	N5
37009_at	AL035079	CAT	38	1.7	N5
37272_at	X57206	ITPKB	39	1.7	N5
31637_s_at	X72631	NR1D1 /// THRA	40	1.7	N5
35693_at	AF070616	HPCAL1	41	1.7	N5
36804_at	M34455	INDO	42	1.7	N5
700_s_at	HG371-HT26388	- ^a	43	1.7	N5
32561_at	D63480	KIAA0146	44	1.6	N0
36023_at	AI864120	-	45	1.6	N0
38783_at	J05581	MUC1	46	1.6	N5
927_s_at	J05582	MUC1	47	1.6	N5
36851_g_at	U42360	TUSC3	48	1.6	N0
35337_at	AL050254	FBXO7	49	1.6	N5
49541_at	X01630	ASS1	50	1.6	N5

^aAn official gene name is not given.

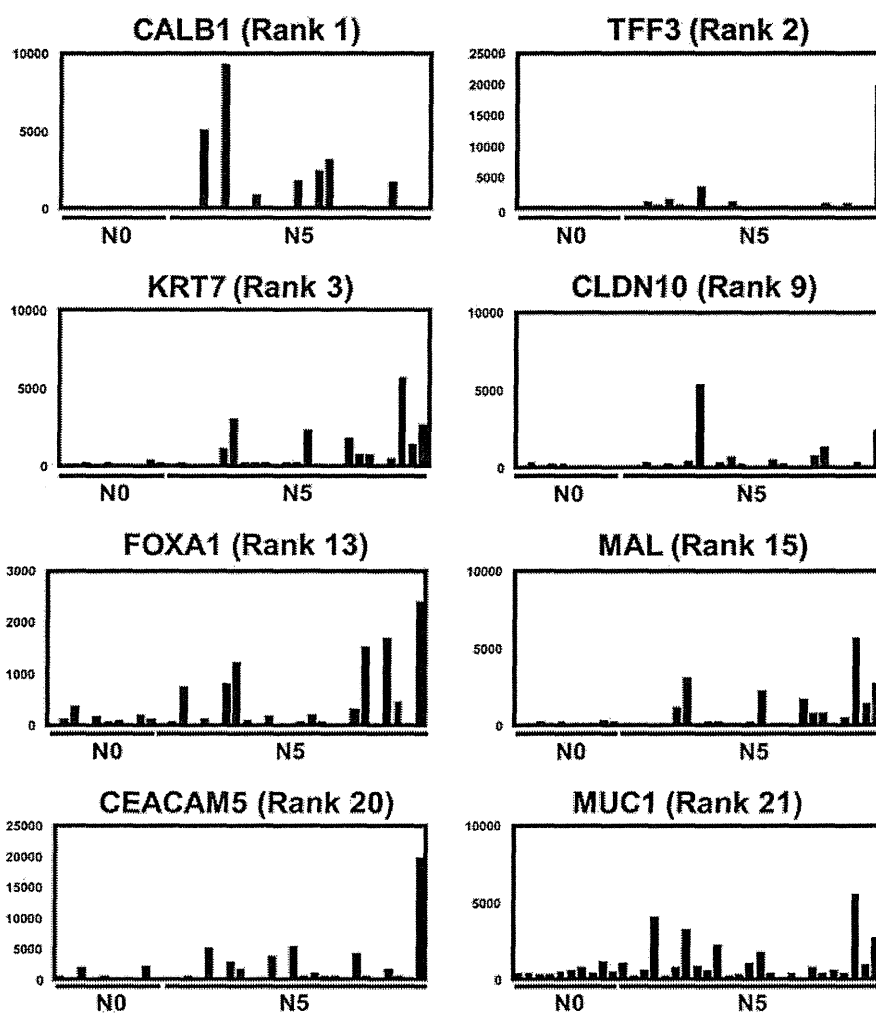


Figure 2. Each signal of microarray for 8 representative top genes whose level was highly correlated with N5 group, respectively.

(10 patients with no metastatic lymph node and 11 patients with >5 metastatic lymph nodes). Similar to the 11 N0 patients and the 24 N5 patients (Fig. 1), Kaplan-Meier analyses of the two groups in each set showed a significant difference in survival after surgical resection (data not shown). In correspondence with microarray data, preferential expression of all the 6 genes in the N5 ESCC patients with >5 lymph nodes was confirmed in the first set (Fig. 3A). Among these 6 genes, 4 (*CALB1*, *KRT7*, *MUC1* and *CEA*) showed a reproducible expression pattern in the second set (Fig. 3B). These 4 genes preferentially expressed in patients with >5 metastatic lymph nodes in both of the two sets of samples. These results suggest that *CALB1*, *KRT7*, *MUC1* and *CEA* are potential molecular markers for ESCC with poor prognosis, and that the present gene list should provide other marker genes. Among the 6 candidate marker genes identified here, *KRT7* seemed to be one of the two best markers, *KRT7* and *CEA* for ESCC with poor prognosis, because it expressed in a few of the 22 patients with no metastatic lymph node, but in >50% of 42 patients with >5 metastatic lymph nodes (semi-quantitative RT-PCR in Fig. 3A and B). These results were confirmed by quantitative real-time RT-PCR (Fig. 3C and D).

Biological implications of the candidate marker genes for ESCC with poor prognosis. Among the 6 genes, *CEA* and *TFF3* were known not to be expressed in the squamous epithelium of the esophagus, skin and uterine cervix, but in the non-malignant or malignant glandular epithelium of the stomach and colon (17). Accordingly, a subset of poor prognostic ESCC is thought to express glandular epithelial cell markers. To confirm this hypothesis, we investigated the expression of *PGC*-encoding pepsinogen C and *LIPF*-encoding gastric lipase that are well-known as typical markers for glandular epithelium of the stomach. Three patients with >5 metastatic lymph nodes (2 in the first set and 1 in the second set) expressed both *PGC* and *LIPF*, clearly (Fig. 4A and B). The percentage in 42 patients with >5 metastatic lymph nodes was 7% (3/42). Interestingly, a patient positive with these two stomach markers (Fig. 4A, lane 42) had the most metastatic lymph nodes (49 positive nodes) among the 64 ESCC patients examined.

KRT7 has been reported to be expressed in the ducts of many tissues including the liver, kidney, pancreas and mammary gland (18); however, relating to esophagus, little is known. As shown in Fig. 4C, immunohistochemical analyses showed that *KRT7* was expressed in the ducts, but not in the

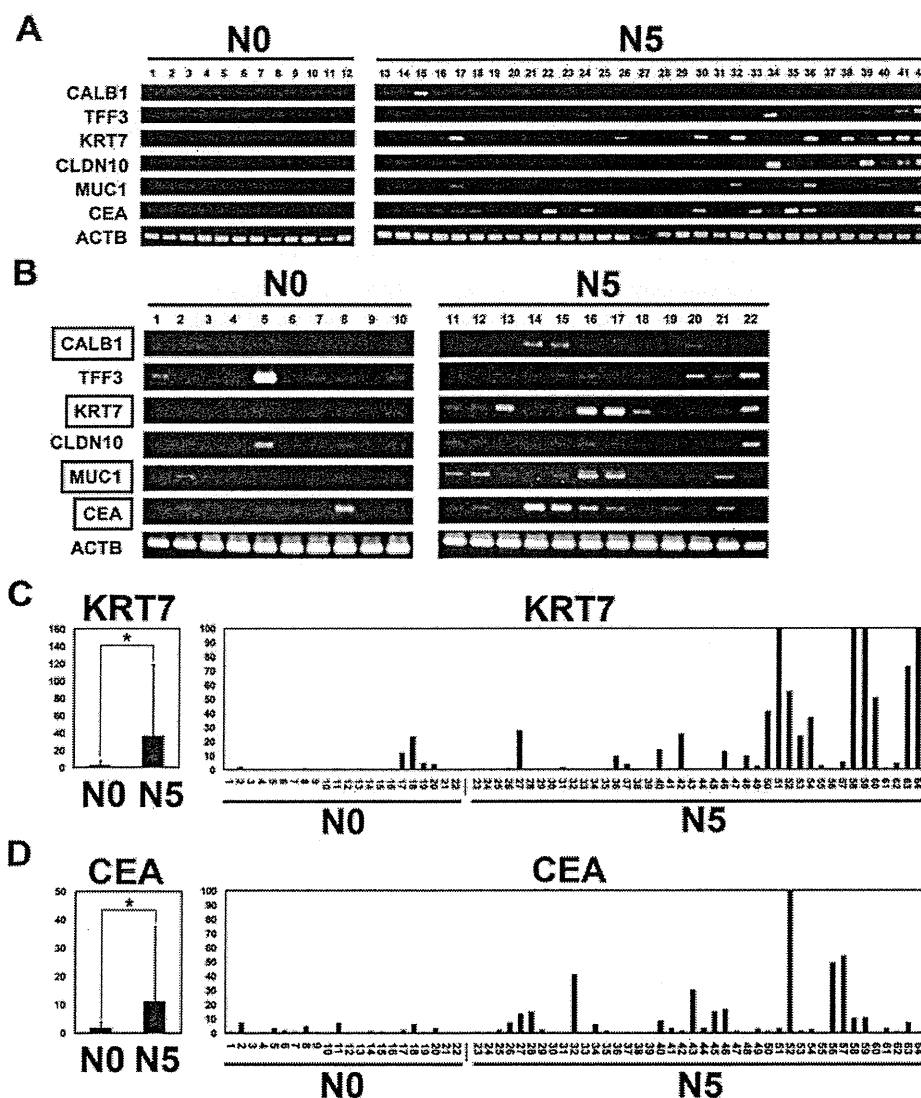


Figure 3. RT-PCR analyses of 6 candidate marker genes for poor prognostic ESCCs with >5 metastatic lymph nodes. (A) Semi-quantitative RT-PCR of 6 poor prognosis marker gene candidates (*CALB1*, *TFF3*, *KRT7*, *CLDN10*, *MUC1* and *CEA*, respectively) in 12 ESCCs with no metastatic lymph node (N0) and in 30 ESCCs with >5 metastatic lymph nodes (N5). (B) Semi-quantitative RT-PCR of these 6 genes in another set of ESCCs consisting of 10 ESCCs with no metastatic lymph node (N0) and in 12 ESCCs with >5 metastatic lymph nodes (N5). Three genes that showed preferential expression in patients with N5 in both the sets of ESCCs are indicated by boxes. (C) Quantitative real-time RT-PCR of *KRT7* in a total of 64 ESCCs consisting of 22 ESCCs with no metastatic lymph node (N0) and in 42 ESCCs with >5 metastatic lymph nodes (N5). (D) Quantitative real-time RT-PCR of *CEA* in these 64 ESCCs. The mean in all samples is indicated by a dotted line.

stratified epithelia of the esophagus. Therefore, *KRT7* could be a marker of the esophageal ducts. Those results suggested that a small subset of ESCCs with poor prognosis expressed some markers of the glandular epithelial cell of the stomach, and that a large subset of the ESCCs with poor prognosis showed a feature of the ducts in the esophagus. We next carefully compared the morphological differences between 13 node negative cases and 19 node positive cases (>5 metastatic lymph nodes). In this morphological study, two expert pathologists examined the slides that were prepared by the other pathologist without information on the nodal status. Percentages of the cases with partial glandular structure in each group were averaged. Interestingly, in accordance with the above-mentioned glandular-epithelial cell marker expression in poor prognostic node-positive

cases, the partial glandular structure was found preferentially in node-positive cases (74%) compared with node-negative cases (38%) (Fig. 4D).

Forkhead box A1 (FOXA1) is an upstream regulator of *KRT7* and *LOXL2* is expressed in a subset of poor prognostic ESCC patients. Although *KRT7* was found to be one of the useful markers for poor prognostic ESCCs, the reason why *KRT7*-overexpressing ESCCs are poor is still unknown. We next searched the upstream transcriptional regulator of *KRT7* in the gene list as shown in Table I and found *FOXA1* as a transcriptional factor co-expressed with *KRT7* (Fig. 2). To investigate whether *FOXA1* is an upstream regulator for *KRT7*, we introduced siRNA of *FOXA1* and *KRT7* into an esophageal cancer cell line, TE3, that has been confirmed to

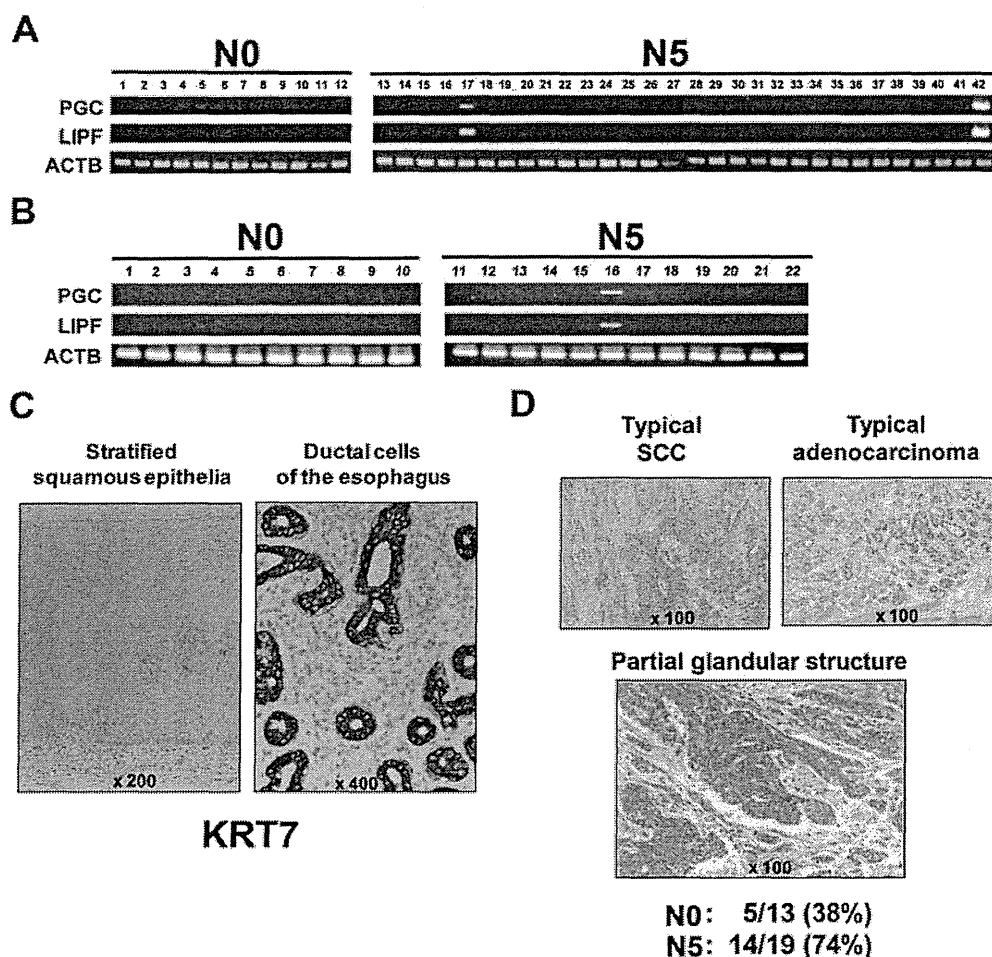


Figure 4. Poor prognostic ESCCs showed characteristics of glandular and/or ductal epithelial cells. (A) RT-PCR of 2 stomach glandular epithelial cell markers (*PGC* and *LIPF*) in the first set of ESCCs. (B) RT-PCR of these 2 stomach glandular epithelial cell markers in the second set of ESCCs. (C) Immunohistochemical staining of KRT7 in normal stratified squamous epithelia and ductal cells in the esophagus. KRT7 is expressed only in ductal cells of the esophagus. (D) Comparison of morphology between N0 and N5 cases. Partial glandular structure was observed preferentially in N0 cases (38%) compared with N5 cases (74%). A typical squamous cell carcinoma (SCC) and adenocarcinoma in the esophagus are shown as a reference (upper).

maintain the expression profile of primary ESCCs the most among 5 cell lines (16) and to express these two genes (data not shown). In this *in vitro* culture, *FOXA1* siRNA successfully reduced the mRNA level of both *FOXA1* and *KRT7*, while *KRT7* siRNA decreased only its own mRNA level (Fig. 5A). We next investigated whether *in vivo* co-expression between *FOXA1* and *KRT7* is observed in primary ESCCs by semi-quantitative RT-PCR. Nine (lanes 16, 17, 22, 34, 36, 39, 40, 41 and 42, respectively) (60%) out of 15 *KRT7* expressing ESCCs with >5 metastatic lymph nodes showed *FOXA1* expression (Fig. 5B). These results suggest that *FOXA1* is an upstream regulator for *KRT7* in a subset of poor prognostic ESCCs.

We next performed genome-wide screening of *FOXA1* downstream genes by microarray analysis of *FOXA1* siRNA-transfected TE3 cells, and found that reduced *LOXL2* expression corresponded to a decrease of *FOXA1* mRNA. This result suggests that *FOXA1* regulates *LOXL2* expression, which was recently reported as a new poor prognosis marker of laryngeal SCCs (19). To confirm the microarray result, we performed quantitative real-time RT-PCR after transfection

of control and *FOXA1* siRNAs into TE3 cells. A significant decrease of *LOXL2* mRNA was found by *FOXA1* siRNA compared with control siRNA (Fig. 5C, left panel). In accordance with the initial *in vitro* study of breast cancer cells (20,21), *LOXL2* siRNA inhibited TE3 cell invasion in Matrigel (Fig. 5C, right panel). We examined the *LOXL2* mRNA expression in primary ESCCs by quantitative real-time RT-PCR. Overexpression of *LOXL2* was observed preferentially in ESCCs with >5 metastatic lymph nodes (Fig. 5D). Five (No. 17, 36, 40, 41, 42) (33%) out of 15 *KRT7* expressing ESCCs with more than 5 metastatic lymph nodes showed both *FOXA1* and *LOXL2* expression (Fig. 5B and D). To this end, we investigated whether *FOXA1* is also involved in cell migration by wound healing assay. As shown in Fig. 6, *FOXA1* siRNA strongly inhibited TE3 cell migration compared with control siRNA. This effect on of the *FOXA1* siRNA treatment was confirmed not to be dependent on growth inhibition of the treatment (data not shown).

Taken together, this study suggests that *FOXA1* induces not only *KRT7* but also *LOXL2* in a subset of poor prognostic

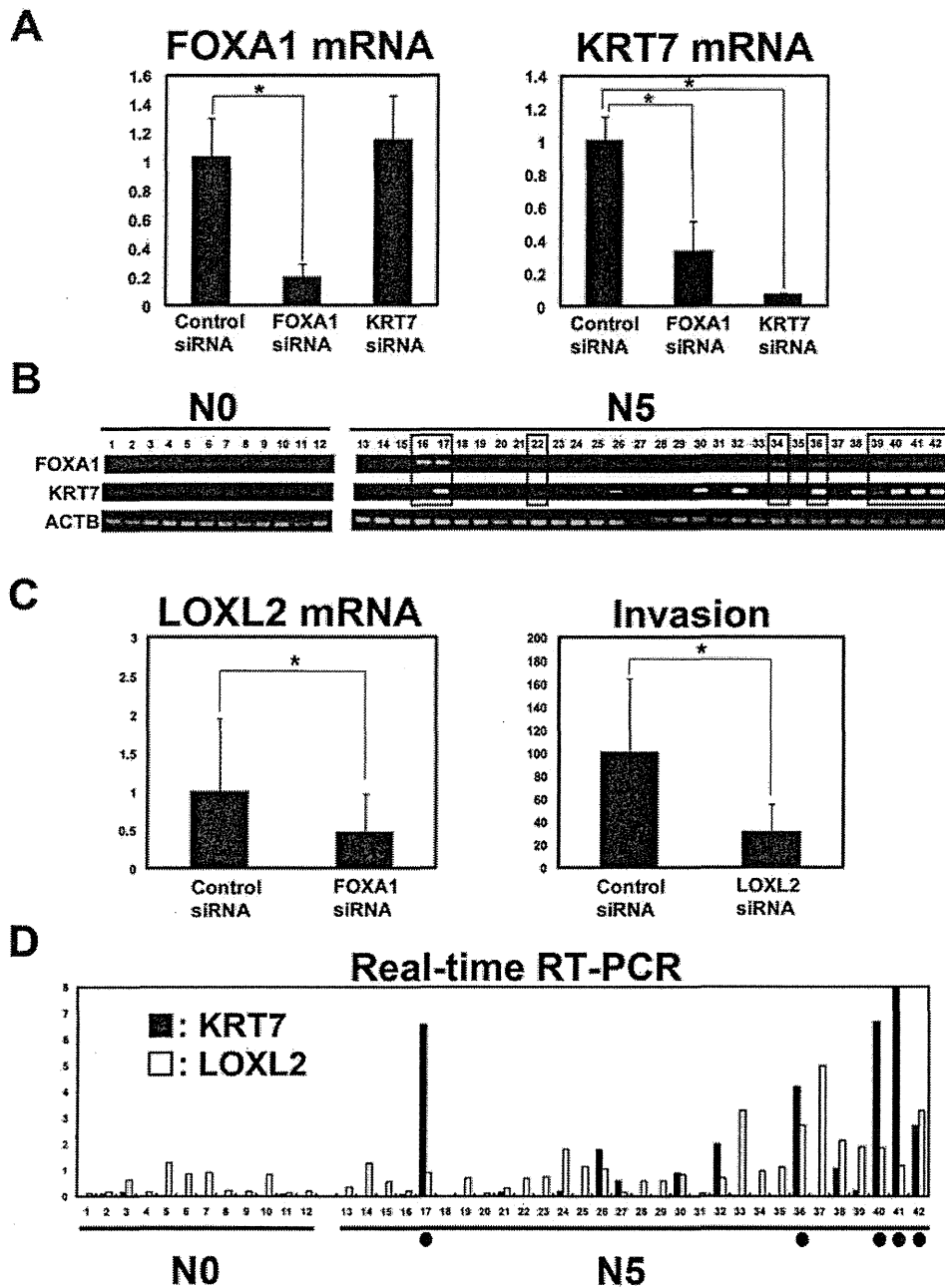


Figure 5. FOXA1 is an upstream regulator of *KRT7* and *LOXL2* in a subset of poor prognostic ESCCs. (A) *FOXA1* siRNA-transfected TE3 cells show reduction of both *FOXA1* and *KRT7* mRNA. Effects on *FOXA1* mRNA (left panel) and *KRT7* mRNA (right panel) after siRNA transfection. (B) Semi-quantitative RT-PCR for showing *in vivo* co-expression between *FOXA1* and *KRT7* in primary ESCCs with poor prognosis. Nine (60%) out of 15 *KRT7*-expressing ESCCs with >5 metastatic lymph nodes show *FOXA1* expression (box). (C) *LOXL2* is another target of *FOXA1* in TE3 cells, and is involved in cell invasion. *FOXA1* siRNA-transfected TE3 cells show reduction of *LOXL2* mRNA (left panel). *LOXL2* siRNA treatment inhibits migration of TE3 cells compared with control siRNA (NC). (D) Overexpression of *LOXL2* in primary ESCCs with >5 metastatic lymph nodes is confirmed by quantitative real-time RT-PCR. Cases with co-expression between *KRT7* and *LOXL2* are indicated by closed circle.

ESCCs with metastatic lymph nodes, and that other FOXA1 downstream genes could be therapeutic targets of poor prognostic ESCCs.

Discussion

Based on our present results, we could divide *KRT7*-expressing ESCCs with >5 metastatic lymph nodes into three

subgroups (Fig. 7). *KRT7* was found to be overexpressed in 15 (50%) of 30 poor prognostic ESCCs with >5 metastatic lymph nodes (Fig.3A). Out of the 15 *KRT7*-overexpressing ESCCs with poor prognosis, 9 cases (60%) showed *FOXA1* expression (Fig. 5B). Therefore, transcriptional factors other than *FOXA1* (as TFs shown in Fig. 7) must activate *KRT7* and metastasis-associated genes (as Xs shown in Fig. 7) in the 6 remaining cases with *KRT7* over-

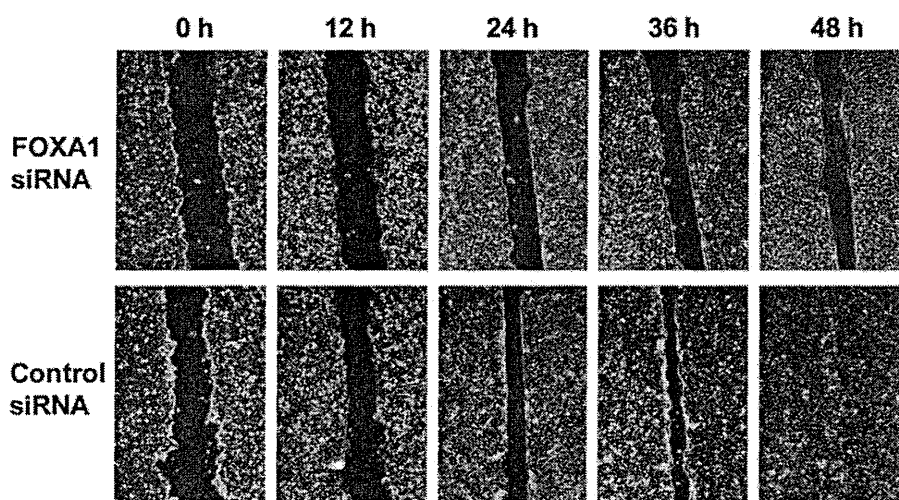


Figure 6. TE3 cell migration after *FOXA1* siRNA treatment. Scratch wound healing assays were performed on TE3 cells after *FOXA1* siRNA and control siRNA transfection. Phase contrast images (original magnification x40) of wound closure at 0, 12, 24, 36 and 48 h, respectively are shown.

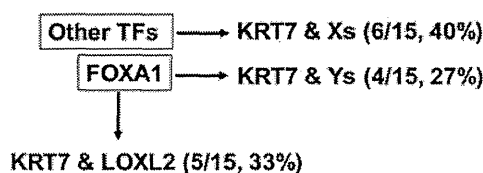


Figure 7. Three subgroups of *KRT7*-expressing ESCCs with poor prognosis. Fifteen of 30 ESCCs with >5 metastatic lymph nodes expressed *KRT7*. The *KRT7*-expressing ESCCs could be divided into three subgroups by the presence of different transcriptional cascades regulating *KRT7*. TFs, transcription factor regulating *KRT7* other than *FOXA1*, and Xs and Ys, metastasis-associated genes other than *LOXL2*.

expression (40%). In five (33%) of the 15 poor prognostic ESCCs, *FOXA1* may regulate both *KRT7* and *LOXL2* (Fig. 5D). Therefore, *FOXA1* must activate not only *KRT7* but also metastasis-associated genes other than *LOXL2* (as Ys shown in Fig. 7) because both *FOXA1* and *LOXL2* are shown to be involved in cell invasion and migration (Figs. 5 and 6).

In accordance with our results, immunohistochemical studies recently revealed that both *LOXL2* and *KRT7* are poor prognosis markers of squamous cell carcinomas including ESCCs (22,23). We also recently reported a map of crosstalk between Hedgehog and EMT signaling in ESCCs (16). *LOXL2* has been reported to stabilize an EMT regulator *SNAI1/SNAI1* through physical interaction on the *SLUG* domain and *Snail*'s lysine residues K98 and K137 (19). In ESCCs, the expression of this EMT regulator should be analyzed in the near future.

The presence of the variable transcriptional cascade in ESCCs may be one of the reasons why a robust gene set, which expresses in association with the prognosis of ESCC patients, could not be extracted by conventional t- or u-test. On this point, our introduced statistical method (S2N') could contribute to the extraction of some genes associated with poor prognosis. However, to understand the molecular

mechanisms in lymph node metastasis and to develop a diagnostic method for all the ESCC patients with poor prognosis, the Xs and their upstream transcriptional factors and Ys should be identified. Chromatin immunoprecipitation (ChIP) -on-chip analysis is a potential tool for identifying *in vivo* direct interaction of the target gene promoter with *FOXA1*. Recently, genome-wide mapping of *FOXA1* targets by ChIP-on-chip analysis revealed that *FOXA1* translates epigenetic signatures into enhancer-driven lineage-specific transcription and its binding consensus sequences in breast and prostate cancer (24). As shown in Fig. 3, poor prognostic ESCCs often seemed to have glandular cell-type characteristics in both the gene expression and morphology. This fact of transdifferentiation from squamous cell to glandular cell may correspond with cell lineage-specific functions of *FOXA1* (24). We were able to find the binding sequences of *FOXA1* at -2630 to -2635 (TAGTTTG) of *KRT7* and at -4530 to -4524 (TGTTTAC), -4304 to -4299 (TGTTTGT), -4300 to -4295 (TGTTTGG), and -2642 to -2636 (TGTTTAC) of *LOXL2*. Future studies on the ChIP-on-chip assay with an anti-*FOXA1* antibody may contribute to an understanding of the malignancy of ESCCs and to the identification of therapeutic targets. In addition, we showed that aside from *KRT7*, other markers for ESCCs with poor prognosis could be *CALB*, *MUC1* and *CEA* (Fig. 3). Therefore, identification of their upstream transcriptional regulators also remains for future studies.

Acknowledgements

This study was supported in part by the program for promotion of Fundamental Studies in Health Sciences of the National Institute of Biomedical Innovation; a Grant-in-Aid for the Third Comprehensive 10-Year Strategy for Cancer Control and for Cancer Research (20-12) from the Ministry of Health, Labour and Welfare of Japan; Princess Takamatsu Cancer Research Fund, and Foundation for Promotion of Cancer Research (RRs: M.S. and T.M.).

References

1. Ando T, Suguro M, Hanai T, Kobayashi T, Honda H and Seto M: Fuzzy neural network applied to gene expression profiling for predicting the prognosis of diffuse large B-cell lymphoma. *Jpn J Cancer Res* 93: 1207-1212, 2002.
2. Parkin DM, Bray F, Ferlay J and Pisani P: Estimating the world cancer burden: Globocan 2000. *Int J Cancer* 94: 153-156, 2001.
3. Ishikura S, Nihei K, Ohtsu A, Boku N, Hironaka S, Mera K, Muto M, Ogino T and Yoshida S: Long-term toxicity after definitive chemoradiotherapy for squamous cell carcinoma of the thoracicesophagus. *J Clin Oncol* 21: 2697-2702, 2003.
4. Igaki H, Kato H, Tachimori Y, Sato H, Daiko H and Nakanishi Y: Prognostic evaluation for squamous cell carcinomas of the lower thoracic esophagus treated with three-field lymph node dissection. *Eur J Cardiothorac Surg* 19: 887-893, 2001.
5. Golub TR, Slonim DK, Tamayo P, Huard C, Gaasenbeek M, Mesirov JP, Coller H, Loh ML, Downing JR, Caligiuri MA, Bloomfield CD and Lander ES: Molecular classification of cancer: class discovery and class prediction by gene expression monitoring. *Science* 286: 531-537, 1999.
6. Tusher VG, Tibshirani R and Chu G: Significance analysis of microarrays applied to the ionizing radiation response. *Proc Natl Acad Sci USA* 98: 5116-5121, 2001.
7. Tibshirani R, Hastie T, Narasimhan B and Chu G: Diagnosis of multiple cancer types by shrunken centroids of gene expression. *Proc Natl Acad Sci USA* 99: 6567-6572, 2002.
8. Takahashi H, Kobayashi T and Honda H: Construction of robust prognostic predictors by using projective adaptive resonance theory as a gene filtering method. *Bioinformatics* 21: 179-186, 2005.
9. Takahashi H, Aoyagi K, Nakanishi Y, Sasaki H, Yoshida T and Honda H: Classification of intramural metastases and lymph-node metastases of esophageal cancer from gene expression based on boosting and projective adaptive resonance theory. *J Biosci Bioeng* 102: 46-52, 2006.
10. Takahashi H and Honda H: Lymphoma prognostication from expression profiling using a combination method of boosting and projective adaptive resonance theory. *J Chem Eng Jpn* 39: 767-771, 2006.
11. Takahashi H, Nemoto T, Yoshida T, Honda H and Hasegawa T: Cancer diagnosis marker extraction for soft tissue sarcomas based on gene expression profiling data by using projective adaptive resonance theory (PART) filtering method. *BMC Bioinformatics* 7: 399, 2006.
12. Takahashi H and Honda H: Modified signal-to-noise: a new simple and practical gene-filtering approach based on the concept of projective adaptive resonance theory (PART) filtering method. *Bioinformatics* 22: 1662-1664, 2006.
13. Takahashi H, Murase Y, Kobayashi T and Honda H: New cancer diagnosis modeling using boosting and projective adaptive resonance theory with improved reliable index. *Biochem Eng J* 33: 100-109, 2007.
14. Kawamura T, Takahashi H and Honda H: Proposal of new gene filtering method, BagPART, for gene expression analysis with small sample. *J Biosci Bioeng* 105: 81-84, 2008.
15. Eisen MB, Spellman PT, Brown PO and Botstein D: Cluster analysis and display of genome-wide expression patterns. *Proc Natl Acad Sci USA* 95: 14863-14868, 1998.
16. Isohata N, Aoyagi K, Mabuchi T, Daiko H, Fukaya M, Ohta H, Ogawa K, Yoshida T and Sasaki H: Hedgehog and epithelial-mesenchymal transition signaling in normal and malignant epithelial cells of the esophagus. *Int J Cancer* 125: 1212-1221, 2009.
17. Leung WK, Yu J, Chan FK, To KF, Chan MW, Ebert MP, Ng EK, Chung SC, Malfertheiner P and Sung JJ: Expression of trefoil peptides (TFF1, TFF2, and TFF3) in gastric carcinomas, intestinal metaplasia, and non-neoplastic gastric tissues. *J Pathol* 197: 582-588, 2002.
18. Smith FJD, Porter RM, Corden LD, Lunny DP, Lane EB and McLean WHI: Cloning of human, murin, and marsupial keratin 7 and a survey of K7 expression in the mouse. *Biochem Biophys Res Commun* 297: 818-827, 2002.
19. Peinado H, del Carmen M, La Cruz I-D, Olmeda D, Csiszar K, Fong KSK, Vega S, Nieto MA, Cano A and Portillo F: A molecular role for lysyl oxidase-like 2 enzyme in Snail regulation and tumor progression. *EMBO J* 24: 3446-3458, 2005.
20. Akiri G, Sabo E, Dafni H, Vadasz Z, Kartvelishvily Y, Gan N, Kessler O, Cohen T, Resnick M, Neeman M and Neufeld G: Lysyl oxidase-related protein-1 promotes fibrosis and tumor progression in vivo. *Cancer Res* 63: 1657-1666, 2003.
21. Kirschmann DA, Seftor EA, Fong SF, Nieva DR, Sullivan CM, Edwards EM, Sommer P, Csiszar K and Hendrix MJ: A molecular role for lysyl oxidase in breast cancer invasion. *Cancer Res* 62: 4478-4483, 2002.
22. Peinado H, Moreno-Bueno G, Hardisson D, Perez-Gomez E, Santos V, Mendiola M, de Diego JI, Nistal M, Quintanilla M, Portillo F and Cano A: Lysyl oxidase-like 2 as a new poor prognosis marker of squamous cell carcinomas. *Cancer Res* 68: 4541-4550, 2008.
23. Yamada A, Sasaki H, Aoyagi K, Sano M, Fujii S, Daiko H, Nishimura M, Yoshida T, Chiba T and Ochiai A: Expression of cytokeratin 7 predicts survival in stage I/IIA/IIB squamous cell carcinoma of the esophagus. *Oncol Rep* 20: 1021-1027, 2008.
24. Lupien M, Eeckhoutte J, Meyer CA, Wang Q, Zhang Y, Li W, Carroll JS, Liu XS and Brown M: FoxA1 translates epigenetic signatures into enhancer-driven lineage-specific transcription. *Cell* 132: 958-970, 2008.

A case of vaginal clear cell adenocarcinoma complicated with congenital anomalies of the genitourinary tract and metanephric remnant without prenatal diethylstilbestrol exposure

Takashi Uehara¹, Takashi Onda¹, Yuko Sasajima², Morio Sawada¹ and Takahiro Kasamatsu¹

¹Gynecology Division, and ²Diagnostic Pathology Division, National Cancer Center Hospital, Chuo-ku, Tokyo, Japan

Abstract

Vaginal clear cell adenocarcinoma (CCA) is well known to be associated with prenatal diethylstilbestrol exposure. We present a vaginal CCA with congenital anomalies of the genitourinary tract without prenatal diethylstilbestrol exposure. A 54-year-old woman complained of a 3-month history of genital bleeding. The examination revealed CCA at the anterior vagina and congenital anomalies. An anterior pelvic exenteration was performed. Macroscopically, bicornuate uterus, vaginal septum and left ureteral agenesis were found. Microscopically, vaginal CCA coexisted with adenosis and both metanephric and mesonephric remnants. The vaginal CCA was supposed to derive from coexisting adenosis. The adenosis was also supposed to occur as a congenital basis, together with genitourinary tract anomalies. Relations between congenital anomalies of the genitourinary tract and vaginal adenocarcinoma were suspected, resultantly.

Key words: clear cell adenocarcinoma, congenital anomaly, diethylstilbestrol, metanephric remnant, vaginal cancer.

Introduction

Primary vaginal malignant tumors constitute only 1 to 3% of all malignant tumors of the female genital tract. Especially, primary adenocarcinoma is very rare, accounting for 6 to 14% of all vaginal malignant tumors.^{1,2} The association of vaginal clear cell adenocarcinoma (CCA) with prenatal diethylstilbestrol (DES)-exposure is well known from the results of numerous extensive investigations. Approximately, two-thirds of the patients with vaginal CCA have a history of prenatal DES-exposure.³ Complex congenital anomalies of the genitourinary tract are rare and metanephric remnant is rarely observed in the surgical specimens. We herein report a rare case of vaginal CCA, which was thought to derive from coexisting adenosis without

any prenatal DES-exposure. In addition, metanephric and mesonephric remnants existed simultaneously.

Case Report

A 54-year-old Japanese woman, gravida 4, para 3, complained of a 3-month history of vaginal bleeding. She visited a nearby hospital. A 2–3 cm protruding tumor at the anterior wall of the upper vagina was noted and its biopsy revealed CCA. She was referred to our hospital for further evaluation and treatment. Only a reddish mucosal lesion along the vaginal septum existed based on inspection and palpation. Two cervical ora existed. The cytological examination of the uterine cervix and endometrium revealed no abnormal findings. Further examinations by computed

Received: February 9 2009.

Accepted: July 1 2009.

Reprint request to: Dr Takashi Uehara, (present address) Department of Obstetrics and Gynecology, Chiba University Hospital, 1-8-1 Inohana, Chuo-ku, Chiba 260-8677, Japan. Email: tak-uehara@hospital.chiba-u.jp

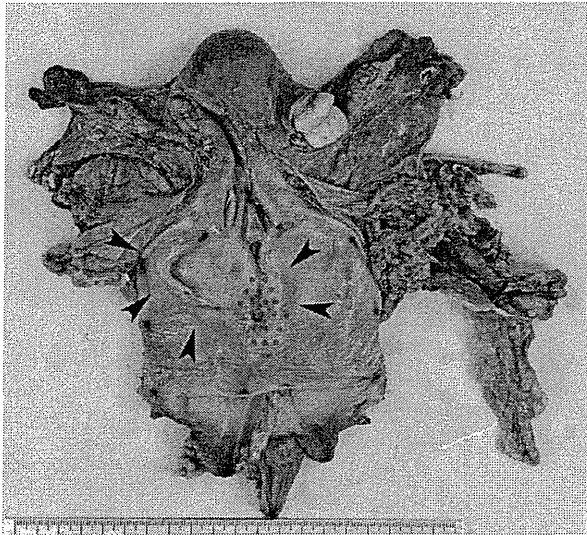


Figure 1 The resected specimen (after formalin embedded). The specimen was opened at the posterior wall of the uterus and vagina. Clear cell adenocarcinoma (dotted area) existed along the anterior vaginal septum (arrow heads). Two cervical ora and endometrial cavities were found. Leiomyoma located at the fundus uteri. The uterus was diagnosed as a bicornuate uterus.

tomographic scan revealed a double inferior vena cava and a left renal agenesis, but no metastasis. She had no history of prenatal DES-exposure.

An anterior pelvic exenteration, a pelvic lymphadenectomy and ileal conduit construction were performed based on a diagnosis of stage I vaginal CCA. Macroscopically, the vaginal septum was present on the left side of the vagina. A reddish mucosal lesion about 1 cm in diameter was present along the septum. The uterus was diagnosed as a bicornuate uterus (Fig. 1). A left ureter was not found in the resected specimen. Microscopically, hobnail type cells constituted invasive small tubules, which were diagnosed to be CCA. This lesion of the CCA was found in the vaginal mucosa along the base of the vaginal septum, and it corresponded to the reddish mucosal lesion recognized on inspection (Fig. 2). The CCA had a tubular or papillary pattern and the tumor cells had coarse hyper-chromatic nuclei with clear cytoplasm (Fig. 3). A tuboendometrial-type adenosis coexisted with surrounding CCA. The adenosis had cilia and a focal squamous metaplasia (Fig. 4). As shown in Figure 2, because the adenosis was surrounded by CCA, the CCA was supposed to arise from the adenosis and surrounded the adenosis. Two long ducts ran parallel from the left

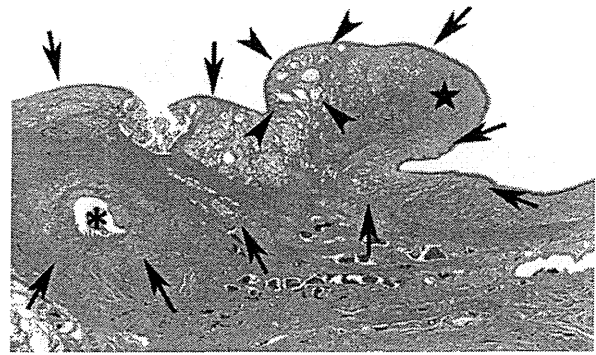


Figure 2 Vaginal septum and clear cell adenocarcinoma (Hematoxylin and Eosin [HE] stain, 2.3 cm in width). Adenosis (arrowheads) existed in the vaginal septum (★) and it was surrounded by clear cell adenocarcinoma (arrows). The metanephric remnant (*) was present in the specimen.

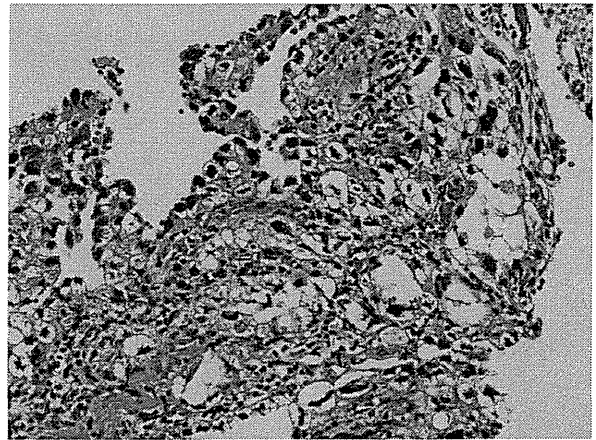


Figure 3 Clear cell adenocarcinoma (HE stain, $\times 200$). Tumor cells demonstrated bizarre nuclei with clear cytoplasm.

side of the uterine cervix to the anterior wall of the vagina. Median and lateral side ducts were thought to be mesonephric and metanephric remnants, respectively (Fig. 5). There was no evidence of endometriosis in the resected specimen. The pathological stage was pT1N0 vaginal CCA. The postoperative course was uneventful. No further treatment was administered as an adjuvant therapy. The patient is presently alive and well without recurrence at 43 months after the surgery.

Discussion

We herein present an exceedingly rare case of vaginal CCA with congenital anomalies of the genitourinary

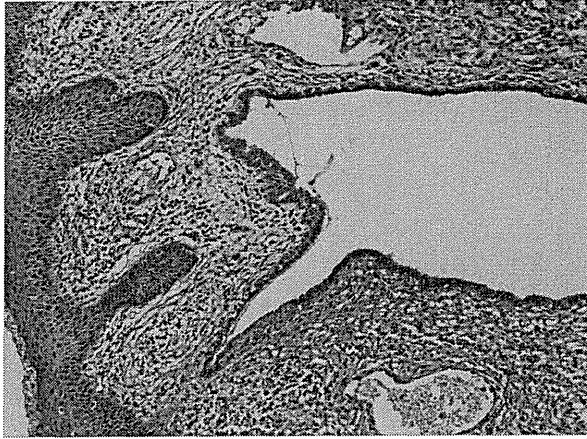


Figure 4 Tuboendometrial-type adenosis in clear cell adenocarcinoma (HE stain, x100). A vaginal stratified squamous epithelium existed on the left side.



Figure 5 Metanephric and Mesonephric remnant (HE stain, x12.5). The clear cell adenocarcinoma invaded into metanephric remnant (left side). The mesonephric remnant was on the right side.

tract without DES-exposure. In addition, both metanephric and mesonephric remnants were microscopically detected. To the best of our knowledge, at least eight similar cases have been reported in the literature (Table 1).⁴⁻¹⁰ The criteria for selecting these cases are: vaginal or cervical adenocarcinoma, especially CCA, macroscopic congenital anomalies of the urinary tract and/or the genital tract, and no history of DES-exposure *in utero*.

In DES-exposed women, DES induces a persistence of embryonic Müllerian epithelium while also

Table 1 Vaginal or cervical adenocarcinoma with congenital anomalies of the genital and/or urinary tract without prenatal DES exposure

Authors	Age	Site	Cancer	Adenosis	Uterine anomaly	Urinary tract anomaly	Other anomaly	Treatment	Outcome
Uehara <i>et al.</i>	54	vagina	CCA	exist	bicornuate uterus	left renal agenesis	metanephric and mesonephric remnant, vaginal septum	APE	NED (43M)
Oht <i>et al.</i>	17	vagina	CCA	not found	ns	left hypoplastic kidney, ectopic ureter	Gartner's duct	RAH+p-VG+RT	ns
Tanaka <i>et al.</i>	17	vagina	CCA	ns	bicornuate uterus	ns	chromosomal anomaly duplicated and imperforated vagina	CT	CR
Satou <i>et al.</i>	38	vagina	CCA	exist	didelphys uterus	ns	ns	RAH+CT	DOD (16M)
Ray <i>et al.</i>	38	vagina	Adenoca.	exist	previously HT	bilateral duplicated ureters	ns	PLA+ILA+RT	NED
Shimao <i>et al.</i>	65	vagina	Adenoca.	ns	bicornuate uterus	left renal aplasia	metanephric remnant	RAH+p-VG+PLA	ns
Nordqvist <i>et al.</i>	27	cervix	CCA	not found	double uterus	absence of one kidney	double vagina	RT+WH, p-VG+PLA	NED (16Y)
Nordqvist <i>et al.</i>	34	cervix	CCA	exist	double uterus	absence of left kidney	mesonephric remnant, double vagina	RAH+p-VG	NED (24Y)
Spörri <i>et al.</i>	49	cervix	CCA	ns	bicornuate uterus	left renal agenesis	ns	RAH+p-VG+RT	NED (4.5Y)

Adenoca, Adenocarcinoma; APE, Anterior pelvic exenteration; CCA, Clear cell adenocarcinoma; CR, Complete response; CT, Chemotherapy; DES, diethylstilbestrol; DOD, Died of disease; HT, Hysterectomy; ILA, Inguinal lymphadenectomy; NED, No evidence of disease; ns, not stated; PLA, Pelvic lymphadenectomy; p-VG, partial Vaginectomy; RAH, Radical abdominal hysterectomy; RT, Radiotherapy; WH, Wertheim hysterectomy.